FACULDADE DE ENGENHARIA DA UNIVERSIDADE DO PORTO

Morphing Techniques to Adapt Pelvic Structures

Margarida Gomes Chiote

Mestrado em Engenharia Biomédica

Supervisor: Dra. Maria Elisabete Teixeira da Silva

Co-supervisor: Prof Dr. Marco Paulo Lages Parente

September 11, 2022

Morphing Techniques to Adapt Pelvic Structures

Margarida Gomes Chiote

Mestrado em Engenharia Biomédica

Faculdade de Engenharia da Universidade do Porto

September 11, 2022

Resumo

O prolapso de órgãos pélvicos (POP) é considerado um distúrbio problemático que ocorre quando as estruturas de suporte pélvico falham. É causada por várias razões, sendo as mais comuns a gravidez e o parto vaginal, sendo que ambas podem causar lesões do músculo do pavimento pélvico e do tecido conjuntivo. Uma melhor visualização desta condição é obtida com a modelação computacional. Assim, torna-se possível simular vários resultados clínicos através do desenvolvimento de modelos específicos que reproduzem as características mecânicas e geométricas de uma região anatómica de interesse a partir de imagens biomédicas, destinadas a fins diagnósticos, terapêuticos, ou cirúrgicos. Quando são suficientemente fiáveis, estes modelos podem representar um paciente virtual, podendo assim substituir a avaliação clínica humana em algumas situações.

Hoje em dia, todos os problemas são analisados e resolvidos com a ajuda de programas informáticos que aceleram os cálculos. Para estudar o comportamento biomecânico das estruturas anatómicas é utilizado o MEF (Método dos Elementos Finitos). O desenvolvimento de modelos pélvicos 3D deve ter em consideração a forma da estrutura e a sua resposta biomecânica. Tal comportamento é fortemente influenciado pela sua geometria. A configuração de pré-processamento pode ser muito demorada quando o modelo FE é baseado em imagens reais, particularmente em 3D, e quando a tarefa deve ser replicada várias vezes para aplicações semelhantes.

O objetivo deste estudo é aplicar o algoritmo desenvolvido a uma estrutura anatómica real obtida a partir de imagens reais de ressonância magnética. Para isso, há um grande número de técnicas para adaptar a forma de uma geometria, para este estudo são utilizadas as funções de base radial (RBFs) baseadas em algoritmos de mesh morphing. Este método funciona através da adaptação da forma da geometria com base na atualização das suas posições dos nós.

Abstract

Pelvic organ prolapse (POP) is considered a challenging disorder that occurs when the pelvic support structures fail. It is caused by several reasons, the most common being pregnancy and vaginal birth, both of which can result in pelvic floor muscle and connective tissue injury. An improved visualization of this condition is obtained with computational modeling. It becomes possible to simulate various clinical outcomes by developing specific models that reproduce the mechanical and geometric characteristics of an anatomical region of interest from biomedical images, intended for diagnostic, therapeutic, or surgical purposes. When they are sufficiently reliable, these models can represent a virtual patient, thus being able to replace human clinical evaluation in some situations.

Nowadays, all but the simplest problems are analyzed and solved with the help of computer softwares that speed up calculations. To study the biomechanical behavior of anatomical structures the FEM (Finite Element Method) is used. The development of 3D pelvic models must take into consideration the shape of the structure and its biomechanical response, such behaviour is heavily influenced by its geometry. The pre-processing setup can be very time-consuming when the FE model is based on real images, particularly in 3D, and when the task must be replicated multiple times for similar applications.

The goal of this study is to apply the developed algorithm to a real anatomical structure obtained from real MRI images. For this, there are a great number of techniques to adapt the shape of a geometry, for this study radial basis functions (RBFs) based mesh morphing are used. This method works by adapting the geometry's shape based on the update of its nodes positions. We begin with the extraction of the nodal coordinates required to adapt the structure. To achieve a shape variation, the displacement was applied to each pre-existing node taking into account its boundary conditions, resulting in an updated location of the set of control points.

Acknowledgments

First of all, I would like to express my sincere thanks to Dr. Maria Elisabete Silva, my supervisor, for her constant and unconditional support throughout the development of this project. Her availability and effort was a determining factor for the completion of this document.

I also want to express my thanks to my co-supervisor, Professor Marco Paulo Lages Parente for his contribution and the opportunities provided throughout this project.

I would also like to gratefully acknowledge the funding from project SIM4SafeBirth - NORTE-01- 0145-FEDER- 030062, financed through FCT and project 2021.00077.CEECIND: Computational Biomechanics as a Tool to Improve Current Treatments. This work was supported by FCT, through INEGI, under LAETA, project UIDB/50022/2020 and UIDP/50022/2020.

Last but certainly not least i would like to thank my family and friends. Throughout the elaboration of this work I had the unconditional support from all of them. However, I would like to mention a few in particular for the role they played.

To my parents, Graça and Eugénio, a huge thank you for all the love, unconditional support and the opportunities they provided me, without them none of this would have been possible.

I thank my friends, especially Inês, Ana and Diogo for believing in me, for the affection and encouragement shown to me over time.

Margarida Gomes Chiote

"Out of clutter, find Simplicity. From discord, find Harmony.
In the middle of difficulty lies Opportunity"

Albert Einstein

Contents

List of Figures

List of Tables

Abbreviations

CAD	Computer-Aided Design
FC	Fecal Incontinence
FEM	Finite Element Method
IAP	Intra-abdominal Pressure
LAM	*Levator ani* Muscles
MDRs	Medical Device Reports
MRI	Magnetic Resonance Imaging
OI	Obturator internus
PFD	Pelvic floor disorders
PFDs	Pelvic Floor Dysfunctions
PFMT	Pelvic Floor Muscle Therapy
PFMs	Pelvic Floor Muscles
ROIs	Regions of Interest
UI	Urinary Incontinence

Chapter 1

Introduction

In this chapter, a brief introduction and contextualization of the study will be given, as well as the objectives and motivation that led to its development. The structure of this report will also be presented.

1.1 Background

Pelvic floor disorders (PFD) are a major global condition that impacts hundreds of millions of women worldwide. At least one type of PFD (urinary incontinence, pelvic organ prolapse, or fecal incontinence) has been noted to be prevalent in approximately 46% [1]. Vaginal birth is considered to be one of the major risk factors when it comes to develop one of this conditions. Vaginal delivery is a remarkable phenomenon about which little is understood in terms of biomechanics [2].

Women's bodies undergo considerable changes throughout pregnancy and after childbirth. Swelling of the abdomen associated with fetal growth, as well as weight gain not only around the uterus but throughout the body. In addition, during pregnancy, bone alignment changes, particularly around the pelvis [3].

The pelvic bones' principal role is to transfer loads generated by human weight and gravity during daily activities. Because body weight increases by nearly 10 kg in 40 weeks, this function is even more critical during pregnancy [3]. Such phenomenon is of great interest when it comes to biomechanical studies. To study the biomechanical behaviour of anatomical structures the FEM (Finite Element Method) is used. This method is a numerical technique that aims to determine the structural state of a body, providing approximate solutions to differential equations that model problems that arise in areas such as physics and engineering.

The biomechanical response of a system is heavily influenced by its model's shape. Shape, however, can differ greatly between people or change as a result of aging or disease [4].

The pre-processing setup can be very time-consuming when the FE model is based on real images, particularly in 3D and when the task has to be replicated multiple times for similar applications [5].

This project aims to produce an accurate 3D model by adapting a pre-existing geometry through the use of morphing techniques, thereby facilitating the computational procedure.

1.2 Objectives

The objectives for the study to be produced are outlined in this chapter.

1. Systematic review of the needed anatomical concepts
2. Classification of pelvic floor disorders.
3. Review of some basic concepts of the finite element method
4. Review of mesh morphing algorithms.
5. Use of Pelvimetry to define the landmarks of the pelvis.
6. Definition of the desired nodes to updates in the Abaqus software.
7. Implementation of a MATLAB algorithm to compute new distances between landmarks.
8. Presentation of the obtained results.
9. Discussion of the results.
10. Final remarks and possible future developments.

1.3 Thesis Outline

This report is structured in six chapters. All theoretical concepts necessary for the development of the dissertation in question are presented in this section. The introduction, contextualization and objectives of this report are described in this chapter.

Chapter 2 consists of a literature review divided into two parts. Initially a review is given of anatomical concepts of interest regarding the female pelvic cavity, as well as the dysfunctions associated with this anatomical structure. Furthermore, the fundamental concepts of mesh morphing techniques are discussed, thus providing an introduction to the scope of the proposed study.

Chapter 3 introduces a more practical component of this project, where morphing techniques are presented, as well as the layout of a finite element analysis.

Chapter 4 begins with the methodology designed for the proposed work.

Chapter 5 begins with the presentation of the results obtained with the computational morphing procedure, focusing on the relevant aspects of the study performed. A discussion of the results and possible justifications for the observed facts is also presented.

Finally, chapter 6 presents the most significant conclusions of this study. Some suggestions for possible future work in this area are also addressed.

Chapter 2

The Female Pelvic Cavity

Diagnosis accuracy is tremendously important when it comes to treatment implications. In recent years, MRI (Magnetic Resonance Imaging) has been widely used as a pre-operative evaluation of PFD, therefore, identifying anatomical defects prior to surgery. Correct classification may increase post-surgical success in a subset of patients, lowering the risk of recurrence [6]. Soft tissue contrast resolution is great on MRI, allowing for precise tissue characterisation and better anatomical delineation [7].

In this chapter a literature review of the female pelvic cavity will be presented, anatomical concepts will be discussed as well as the most common identified PFD. Furthermore, some background regarding Magnetic Resonance Imaging is provided, establishing its role in the present study.

2.1 Anatomy of the Female Pelvic Cavity

Communication between interdisciplinary areas such as engineering and medicine is crucial. Thus, the importance of anatomical knowledge of the structures considered relevant is highlighted, as well as the biomechanical properties associated with them.

For a correct interpretation of this document, a review of anatomical concepts is presented. In order to describe the relative positioning of pelvic structures, there are six fundamental directions and three generally considered anatomical planes to take into account [8]:

- Sagittal Plane- plane that divides the body into two parts, left and right.
- Frontal Plane- divides the body into anterior and posterior parts, and may also be called the coronal plane.
- Transverse Plane: divides the body into two parts, upper and lower.

As for the directions, these are:

- Anterior and Posterior- the term anterior refers to the direction that points to the front of the body, contrary to this, the term posterior indicates the direction to the back of the body.

- Superior and Inferior- superior indicates the direction that points to the head, while inferior corresponds to the direction that points to the feet.

- Medial and Lateral- the term medial corresponds to the approach of a structure to the sagittal plane, while the lateral structure refers to a departure from this plane.

These concepts are based on the anatomical reference position, in which the subject is in an upright position with feet together and arms at the side of the body with palms facing the observer [9]. This position along with the reference planes and directions is illustrated in Figure 2.1.

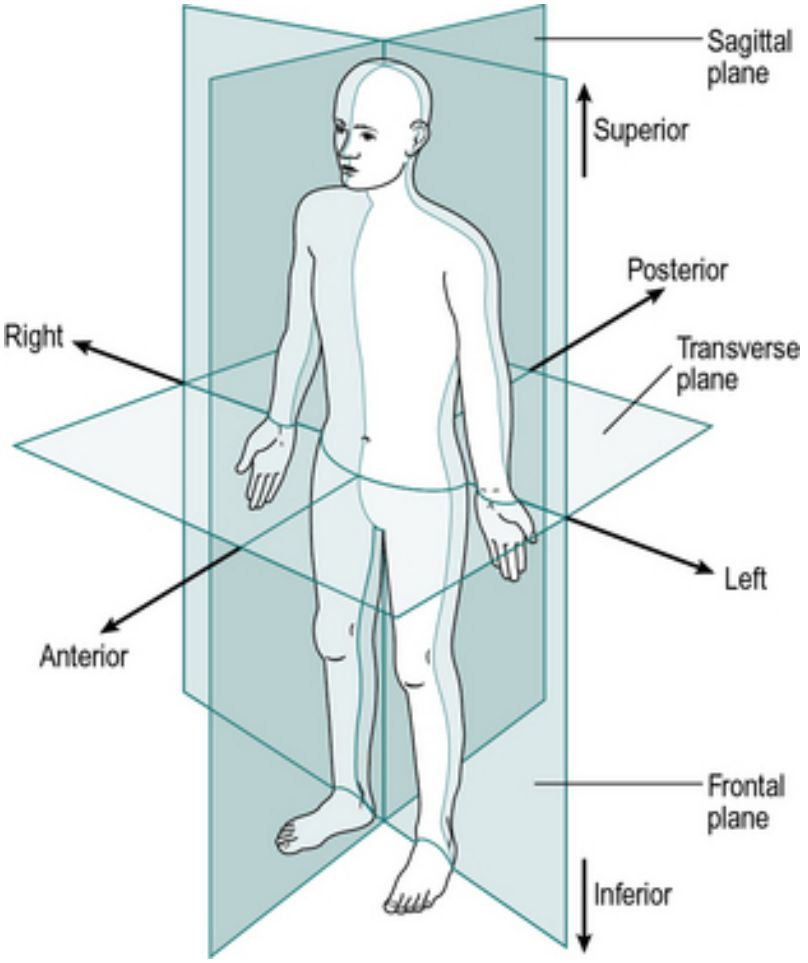

Figure 2.1: The anatomical position, with the three reference planes and six fundamental directions, adapted from [8].

The female pelvic cavity (seen in Figure 2.2) is a bowl-like structure that sits below the abdominal cavity. In females, this structure is composed of a group of organs (uterus, ovaries, bladder and rectum), ligaments, muscles, nerves, and blood vessels which are required for reproduction and the activities of the human excretory system [10, 11]. Knowledge of anatomy unique to females is essential for all clinicians, especially those in the field of obstetrics and gynecology.

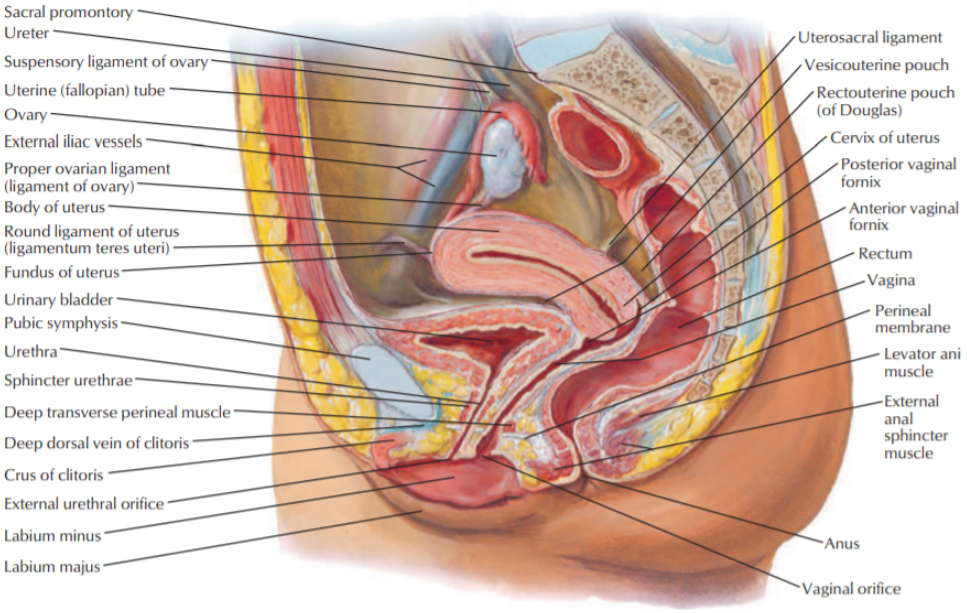

Figure 2.2: Sagittal section of the pelvic floor and pelvic structures, adapted from [12].

2.1.1 Organs of the Female Pelvic Cavity

The organs that belong to the female pelvic cavity can be divided into three categories, which include the urinary organs, the internal genitalia and lastly the rectum and anal canal. All of these structures can be seen in Figure 2.2.

Urinary organs are composed of the **urinary bladder** and the **urethra**. The **urinary bladder** operates as a reservoir and fluctuates in size, shape, position, and relationships depending on the volume of urine held and the state of the surrounding viscera. When empty, this structure is considered the most anterior pelvic organ, and it is totally positioned in the pelvis [10]. The bladder expands superiorly as it distends, crossing the pelvic barrier into the abdominal cavity (false pelvis). It has a fundus, a neck, an apex, a superior and two inferolateral surfaces when empty and is relatively tetrahedral [13].

The female **urethra** is approximately 4 cm long and 6 mm wide. It begins at the bladder's internal urethral opening and runs antero-inferiorly behind the *pubic symphysis*, buried in the vaginal wall [13, 14]. The inner layer of the urethra consists of smooth muscle tissue, and the outer layer of striated muscle (external sphincter), whose fibers are arranged circularly around the urethra, forming a thicker sheath in the middle third of the urethra. The circular configuration implies the constriction of the sphincter allowing for the voluntary control of urinary continence.

The internal genitalia is the structures within the true pelvis, including the **vagina**, **cervix**, **uterus**, **fallopian tubes** and **ovaries**.

The **vagina** is an 8-centimeter long muscular and membranous canal. This structure is located anteriorly to the rectum and posteriorly to the wall of the bladder and urethra. Due to its oblique placement, the anterior wall is somewhat smaller than the posterior wall. The upper segment of the vaginal forms a vaginal vault by being enclosed within the vaginal portion of the **cervix**. The cervix protrudes into the vaginal canal, creating a passageway between the two structures. As a result, the cervix is separated into two parts: supravaginal and vaginal [15].

The **uterus** is a fibromuscular organ of the female reproductive system. It's a thin, closed membrane through which the fetus develops throughout pregnancy. It's pear-shaped, with a length of 7.6 cm, a width of 4.5 cm, and a thickness of 3.0 cm. When pregnant, a woman's uterus will increase from 8 cm long to 35 cm. This structure is composed of two separate parts, the body (connects part of the uterus to the Fallopian tubes) and the cervix (connects the uterus to the vagina) [16].

As mentioned, the **ovaries** are linked to the uterus through the **Fallopian tubes**, which function to carry the zygote to the uterine cavity for implantation. They also help when it comes to bringing the sperm and ovum to this site of fertilization. The ovaries are considered one of the most important organs in the female reproductive system. They lie within the pelvis and are located laterally to the uterus. They sit within the ovarian fossa, in front of the ureters, and behind the external iliac vessels [17].

The **anal canal** is considered an anatomically unique structure with a major complicated physiology, which explains its critical role in continence and susceptibility to a variety of conditions. Continence is preserved trough the tonic circumferential sphincter contraction, enabling the anus and the anal canal to be almost fully closed [18].

The **rectum** is the most distal section of the large intestine, bordered proximally by the sigmoid colon and distally by the anal canal. This structure is located in the pelvis, begins at the level of the sacral promontory, and extends, approximately, 12 to 18 cm distally [19]. The rectum serves as a temporary excrement storage area. It collects feces from the descending colon, which is carried through peristalsis, or regular muscular contractions. Stretch receptors in the rectal walls trigger the need to pass feces as the rectal walls expand due to the contents filling it from within, a process known as defecation [20].

2.1.2 Bony Pelvis

The pelvic floor muscles (PFMs), as well as the pelvis itself (Figure 2.3), provide support for abdominal organs. As a result, the pelvis and its coresponding muscles are at the center of a few clinical disorders that people face today [21].

The skeletal system has the role of protecting the internal organs, to transfer the body weight from the axial skeleton to the appendicular skeleton for standing and walking. In the female,it is also adapted for childbearing. The pelvic cavity is limited anteriorly by the pubis, laterally by the hip bones (ilium and ischium) and posteriorly by the sacrum, which articulates inferiorly with the coccyx [22, 23].

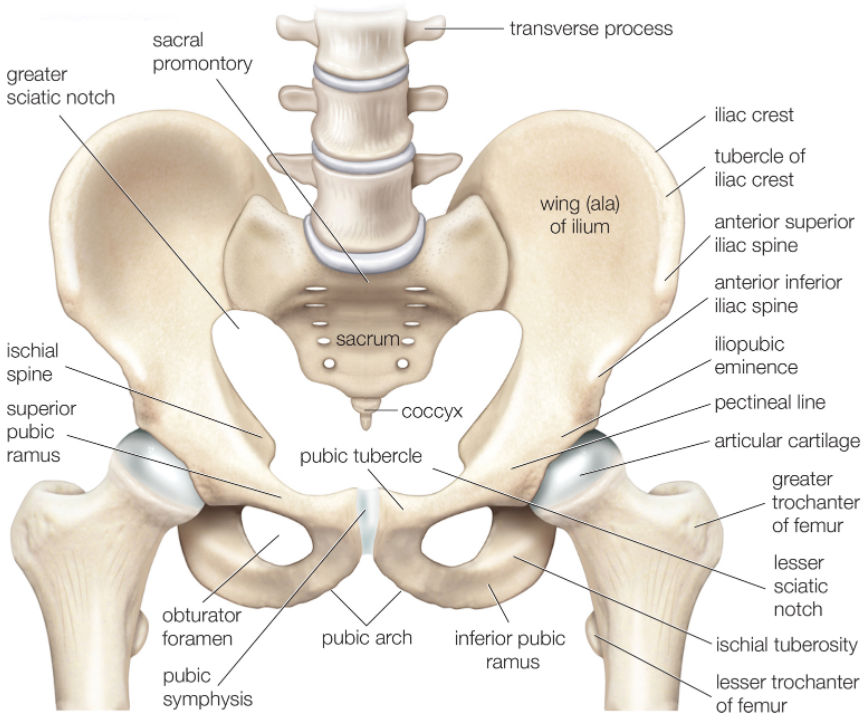

Figure 2.3: Bony landmarks of the pelvis [24].

The pelvis is separated anatomically into two parts: a greater or false pelvis and a lesser or true pelvis. An oblique plane stretching across the pelvic brim from the sacral promontory to the *symphysis pubis* separates the true (lesser) and false (greater) pelvises. In a female, the real pelvic cavity contains the rectum, bladder, pelvic ureters, vagina, uterus, and ovaries. The iliac fossae establish a lateral border to the false pelvis, which is open anteriorly [25].

2.1.3 The Pelvic Floor and Support Structures

Pleasure and sexuality, parturition, urination and urinary continence, defecation and fecal continence, and keeping the pelvic organs in place are all functions of the female pelvic floor. The pelvic floor, which is made up of muscle, connective tissue, and nerves, is required to perform all of these functions [26]. Furthermore, the central nervous system is in charge of its function. Pelvic floor function and continence can be harmed not only by direct anatomical injury (as in vaginal delivery), but also by faulty neural control, as shown in neurologic disease, diabetic neuropathy, and cognitive problems.

2.1.3.1 Pelvic Floor Muscles

The muscles that span the pelvic floor are collectively known as the pelvic diaphragm. In females, the PFMs serve two purposes: they support or act as a "floor" for the abdominal viscera, including the rectum, and they serve as a constrictor or continence mechanism for the urethral, anal, and vaginal orifices [27].

There are two sets of muscles that arise from the pelvis. The first one being the piriformis and obturator internus (OI) muscles that are part of the pelvic walls and are primarily considered lower-limb muscles. The second set of muscles belongs to the pelvic diaphragm, this structure is formed by the *levator ani* (LAM) and *ischiococcygeus* muscles, which define the real pelvis' lower limit. All of the above are labeled in Figure 2.4.

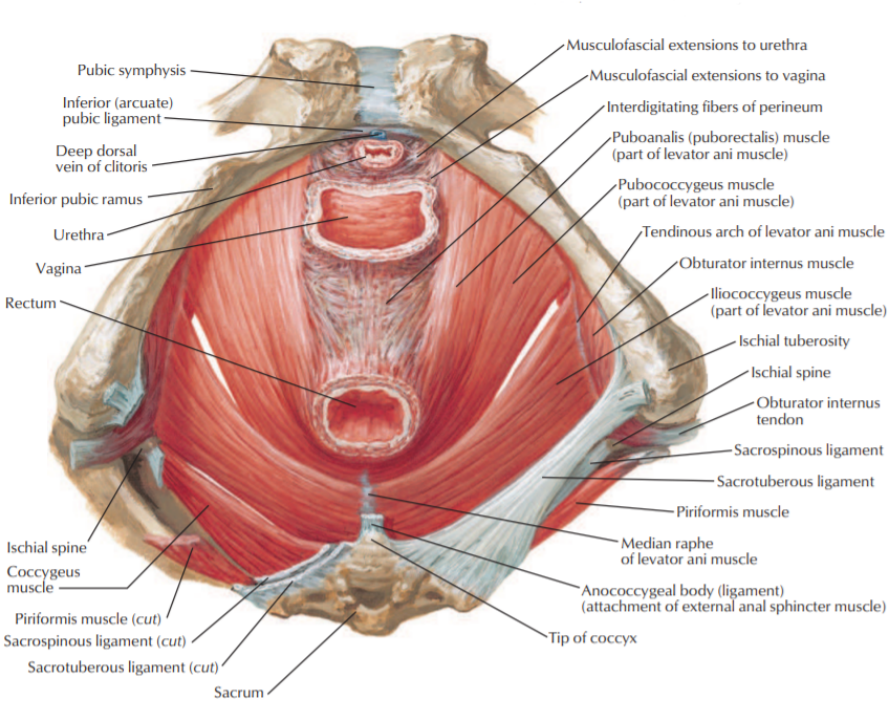

Figure 2.4: Inferior view of the pelvic floor and pelvic structures, adapted from [12].

The **piriformis** muscle slides out of the pelvic cavity just above sacral spinal ligament, under the greater sciatic notch of the coxal bone. It then descends diagonally into the gluteal region, ending on the upper side of the femur's greater trochanter. This muscle is considered a lateral hip rotator that also serves as an extensor [28]. When its point of support on the sacrum is proximal, it may take on a secondary role as an abductor. **Obturator internus** and the fascia over its upper, inner (pelvic), surface form part of the anterolateral wall of the true pelvis [9]. The OI is a lateral rotator of the extended hip and an abductor of the flexed hip. However, as the hip goes from flexion to extension, the OI shortens, showing that it plays a crucial function in providing and maintaining hip stability during weight bearing and propulsive action [9, 29].

LAM muscles form a large section of the pelvic floor, they are divided into three, the *pubococcygeus*, *iliococcygeus* and *puborectalis*. These sections are frequently referred to as different muscles, but the boundaries between them are difficult to discern, and they execute many of the same physiological activities [9, 30].

Pubococcygeus originates from the posterior part of the inferior rami of the pubis and anterior part of the obturator fascia. Furthermore, this muscle controls urine flow, also aids in the reduction of urinary incontinence. A weaker *pubococcygeus* muscle is noted in a higher percentage of urinary incontinence patients, particularly in pregnant and post-pregnant women [31, 32].

The ***iliococcygeus***, the levator's most posterior and thinnest component, serves mostly as a support. The majority of posterior fibres are linked to the sacrum and coccyx's extremities, but the majority unite fibers from the opposing side to produce a raphe that is effectively continuous with the fibroelastic anococcygeal ligament, which is tightly applied to its inferior surface [9, 30].

Puborectalis emerges from the superior fascial layer of the urogenital diaphragm and the inferior section of the *pubic symphysis*. It forms a sling around the rectum, where it meets fibers from the opposing muscle at the midline. When it meets the fibers on the opposite side, it produces a sling around the lower rectum. In the defecation process, it operates in conjunction with the internal and external anal sphincters [31, 32].

Ischiococcygeus is a distinct muscle that is often called coccygeus. It arises as a triangle musculotendinous sheet with its apex connected to the pelvic surface and tip of the ischial spine, and its base attached to the lateral edges of the coccyx and the fifth sacral segment, and it lies as the most posterosuperior component of *levator ani*. Ischiococcygeus is rarely absent, but it present itself tendinous rather than muscular [9].

Table 2.1 summarizes the section that was presented.

Table 2.1: Summary table of the muscles of the pelvic walls and floor, adapted from [33]

Boundary	Muscle	Proximal Attachment	Distal Attachment	Innervation	Main Action
Lateral wall	**Obturator internus**	Pelvic surfaces of the ilium and ischium; obturator membrane	Greater trochanter of the femur	Nerve to obturator internus (L5, S1, S2)	Rotates the thigh laterally; assists in holding the head of the femur in acetabulum
Posterosuperior wall	**Piriformis**	Pelvic surface of S2–S4 segments; superior margin of greater sciatic notch and sacrotuberous ligament	Greater trochanter of the femur	Anterior rami of S1 and S2	Rotates the thigh laterally; abducts the thigh; assists in holding the head of the femur in acetabulum
Floor	**Coccygeus** (ischiococcygeus)	Ischial spine	Inferior end of the sacrum and coccyx	Branches of S4 and S5 spinal nerves	Forms small part of pelvic diaphragm that supports pelvic viscera; flexes coccyx
	Levator ani (puborectalis, pubococcygeus, and iliococcygeus)	Body of pubis; tendinous arch of obturator fascia; ischial spine	Perineal body; coccyx; anococcygeal ligament; walls of the prostate or vagina, rectum, and anal canal	Nerve to levator ani (branches of S4), inferior anal (rectal) nerve, and coccygeal plexus	Forms most of pelvic diaphragm that helps support pelvic viscera and resists increases in intra-abdominal pressure

2.1.3.2 Pelvic Floor Fascias and Ligaments

The endopelvic fascia is a structure formed by connective tissue that connects the bladder and urethra, as well as the vaginal and uterine walls, to the pelvic walls. This structure is one contin-

uous mass that seats beneath the peritoneum, with distinct thickenings or condensations in certain places. The endopelvic fascia is connected to the visceral fascia, which forms a capsule around the organs and allows for volume changes and displacements [30]. Individual names are given to the different sections of this structure, primarily ligaments and fascia, which have a diverse internal structure. Collagen fibers are interlaced with elastin, smooth muscle cells, fibroblasts, and vascular structures in the endopelvic fascia and ligaments, which form a mesh-like structure. The cardinal ligaments, which connect the uterus to the pelvic wall, are made up of supporting collagen that forms the walls of arteries and veins. Other structures, such as the endopelvic fascia's pelvic sidewall attachment (arcus tendineus of the pelvic fascia), are mostly made of fibrous collagen [32].

Pelvic ligaments (Figure 2.5) are structures that result from condensations of the endopelvic fascia, composed of nerves, blood vessels and smooth muscle. Their composition indicates that they are contractile structures and therefore play an important role in supporting the pelvic organs [34, 35].

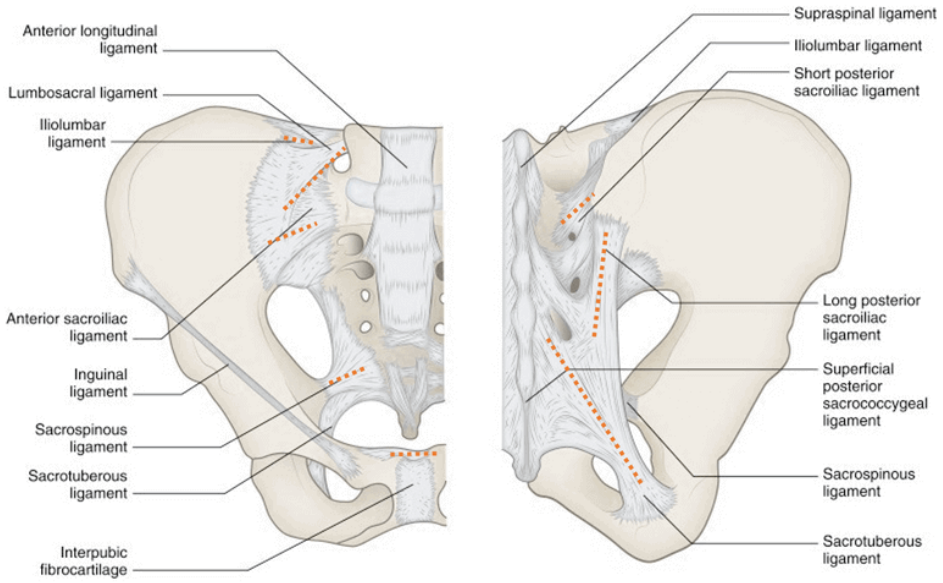

Figure 2.5: The pelvic ligaments, adapted from [36].

According to [34], there are ligaments that stand out because they actively participate in pelvic visceral support and that the lack of their integrity can induce pathological conditions of some dysfunctional pelvic dysfunctions, as can be seen next.

- **Vaginal vault prolapse** – Lack of support or weakness of the uterosacral ligaments, cardinal ligaments, and attachment loss of the endopelvic fascia to the white line at the level of the sacrospinous ligament, or a combination of the above stated causes herniation of the vaginal vault.

- **Uterine prolapse** – The uterus herniates due to a loss of support from the uterosacral and/or cardinal ligaments.
- **Cystocele** – The anterior's wall endopelvic fascia tears, stretches, or a combination of the two causes herniation of the anterior vaginal wall and bladder. A central cystocele can occur from a midline lesion, while a lateral insult can result in a paravaginal abnormality.
- **Enterocele** – The posterior vaginal wall endopelvic fascia tears, stretches, or a combination of the two causes herniation of the superior section of the posterior vaginal wall.
- Rectocele – The posterior vaginal wall endopelvic fascia tears, stretches, or a combination of the two causes herniation of the inferior section of the posterior vaginal wall and rectum.

2.1.3.3 Perineal Membrane

The perineal membrane provides the anatomic support of the distal urethra, distal vagina, and perineal body by attaching these structures to the bony pelvis [37]. The membrane acts as a bridge between the cavity that exists in the *pubis* and the perineal body, allowing the filling of the urogenital opening. It behaves as a sphincter of these same regions contributing to continence [38].

2.1.3.4 Perineal Body

The perineal body (PB) is a pyramidal fibromuscular mass of connective tissue located between the posterior vaginal wall's distal third and the anus. Because the PB helps to maintain the distal vagina and rectum, it's important to focus on reattaching the damaged extremities of the anatomic structures that make up the perineal body during episiotomy repairs and perineal reconstructive surgeries [30, 39].

2.2 Pelvic Floor Dysfunction

As mentioned previously, PFMs have a major role in supporting the organs of the female pelvic cavity. Their dysfunction is a critical component when it comes to pelvic floor disorders (PFDs), which include pelvic organ prolapse (POP), and urinary and fecal incontinence.

The prevalence of PFDs increases significantly with age, this being said, a large proportion of patients seeking treatment for these conditions are older women. [29]. This type of disorders affects hundreds of millions of women worldwide. Approximately 46% percent of women have at least one type of PFD (urinary incontinence (UI), pelvic organ prolapse, or fecal incontinence (FI)) [1].

2.2.1 Pelvic Organ Prolapse

Pelvic organ prolapse (POP) is a gynecological dysfunction that affects women and is caused by rupture or impairment of the pelvic floor suport structures [40]. It occurs when one or more female

pelvic organs, such as the bladder, uterus or rectum, protrude outside the pelvis through the vaginal wall, causing the pelvic organs to drop downward to the vaginal wall [41].

POP might present itself with only one symptom (vaginal bulging or pelvic pressure) or as a collection of symptoms, such as bladder, bowel, and pelvic symptoms [42].

There is a shortage of epidemiological studies about the prevalence and incidence of POP. Only 10 to 20 % of women seek treatment for this problem, despite the fact that it is estimated that roughly 50 % of all women will develop it [43]. The most common causes of POP are pregnancy, aging, childbirth, and previous pelvic surgery. Chronic pulmonary disease, obesity, and physical labor can lead to an increase of the intra-abdominal pressure, thus being considered risk factors when it comes to developing POP [44].

According to The Pelvic Organ Prolapse Quantification system (POPQ) (Table 2.2), POP can be categorized in five stages [45].

Table 2.2: Five stages of pelvic organ support as defined by the POPQ [42].

Stage	**Definition**
0	No sign of prolapse.
I	The most distal part of the prolapse is more than a centimeter above the hymen.
II	The most distal portion of the prolapse is less than or equal to a centimeter proximal or distal to the hymen.
III	The most distal part of the prolapse is more than a centimeter below the hymen but no more than two centimeters further than the total vaginal length.
IV	Complete eversion of the total length of the vagina. Beyond the hymen, the distal part protrudes at least the whole vaginal length minus 2 cm.

In addition to this, POP can also be classified by the structure that is lodged outside its anatomical site (see Table 2.3 and Table 2.4).

Table 2.3: Traditional anatomical site prolapse classification [46].

Type of POP	**Definition**
Urethrocele	Prolapse of the lower anterior vaginal wall involving the urethra only.
Cystocele	Prolapse of the upper anterior vaginal wall involving the bladder. Generally, prolapse of the urethra is also associated and hence the term cystourethrocele is often used.
Uterovaginal Prolapse	This term is used to describe prolapse of the uterus, cervix and upper vagina.
Enterocele	Prolapse of the upper posterior wall of the vagina usually containing loops of small bowel.
Rectocele	Prolapse of the lower posterior wall of the vagina involving the rectum bulging forwards into the vagina.

Table 2.4: Anatomical classification according to vaginal walls, adapted from [46]

<table>
<tr><td rowspan="2">Anterior Vaginal Wall</td><td colspan="2">Cystocele</td><td colspan="2">Urethrocete</td></tr>
<tr><td colspan="2">• Central (Posterior)
• Lateral (Anterior)
• Combined</td><td colspan="2">Uncommon</td></tr>
<tr><td rowspan="2">Apical Vaginal Wall</td><td>Enterocele</td><td>Uterine</td><td>Uterovaginal</td><td>Vaginal Vault</td></tr>
<tr><td>• Anterior
• Posterior</td><td></td><td>With cystocele enterocele, rectocele*</td><td>Eversion (post-hysterectomy) with cystocele, enterocele, rectocele</td></tr>
<tr><td rowspan="2">Posterior Vaginal Wall</td><td colspan="4">Rectocele</td></tr>
<tr><td colspan="4">• Low
• Midvaginal
• High</td></tr>
</table>

2.2.2 Urinary Incontinence

UI in women is usually caused by bladder or pelvic floor muscle failure, which can occur during pregnancy, childbirth, or menopause [47].When there is an increase in intra-abdominal pressure (IA), during the execution of various activities such as coughing and physical activities, there is an increase in the intra-vesical pressure in relation to the urethral pressure producing an involuntary loss of urine.

There are two types of urinary incontinence: stress urinary incontinence, which occurs when urine leaks as a result of physical activity, and urgency urinary incontinence, which occurs when urine leaks as a result of a sudden urgent desire to discharge. Mixed urine incontinence is defined as when a woman experiences both symptoms. The detrusor muscle or pelvic floor muscles (PFMs), malfunction of the brain controls of storage and voiding, and disruption of the local environment within the bladder are all potential causes of incontinence, according to research [47].

2.2.3 Fecal Incontinence

The involuntary loss of feces from the anal canal is referred to as fecal incontinence (FI). This PFD is a physically and emotionally distressing condition that has a significant influence on one's quality of life. It has a profound impact on patients, as well as their families, caregivers, and society as a whole [48]. The loss of anatomical support of the rectum can cause varied degrees of prolapse and rectoceles, which can lead to inefficient or obstructive defecation and fecal incontinence symptoms [49].

2.3 Treatments for Pelvic Floor Dysfunctions

Pelvic floor muscle therapy (PFMT) is widely recommended for PFDs. Through repetitive voluntary contractions of varying intensity and duration, this therapy seeks to increase the function and strength of the PFMs. Kegel exercises have been shown to help with stress urge and mixed incontinence symptoms, and they can also help women with mild POP [50, 51].

Treatment options differ depending on the extent of the prolapse and the symptoms. Simple observation, vaginal pessaries, or surgical management are all options that are taken into consideration. Severe cases of POP require a more invasive approach, available surgical options are reconstructive pelvic surgery with or without mesh augmentation and obliterative surgery [52].

A **vaginal pessary** is a device which is inserted into the vagina to hold a prolapsed womb and/or vaginal walls into place [53]. Pessaries can be made of silicone or vinyl. There are a variety of models that can be chosen for implementation, but the two different types of pessary that are most commonly used are ring and shelf pessaries. This device is used when surgery needs to be avoided, or to control POP symptoms whilst waiting for surgery. It can also be recommended if there's the desire to have children or if surgery may not be a safe option due to other health problems. With its implementation some side effects are observed, the most common being [54, 55]:

- Vaginal discharge with an unpleasant odor, which could indicate a bacterial infection in the vaginal canal (bacterial vaginosis).
- Some vaginal discomfort and blisters, as well as bleeding.
- Urinary tract infection.
- Stress incontinence, where a patient passes a small amount of urine when they cough, sneeze or exercise.

Patients must confirm that the pessary is in the proper location after insertion by completing various activities of daily living (sitting, standing and bending postures, Valsalva maneuver). Within 4 to 6 weeks of pessary placement, all patients should be checked [41].

When the stage of POP is too severe surgery is often required. There are a few different approaches that may be pursued. The integrity of the female reproductive system is often a key factor for this decision. Surgical management options include **surgical repair**, **mesh surgery** and **obliterative surgery**.

Table 3.1 shows all the different types of prolapse. For each type of prolapse there is a corresponding type of surgery that involve lifting and supporting the pelvic organs in question [41]. Pelvic floor repair is considered a broad term used to describe simple **surgical repairs** of the female pelvic floor. More specifically, the term **anterior repair** refers to correction of the front wall of the vagina; and **posterior repair** refers to correction of the back wall of the vagina.

Anterior repair is a surgical treatment that involves restoring or strengthening the damaged tissues between the bladder and the vagina. The surgery's goal is to alleviate the symptoms of

vaginal bulging/laxity while also improving bladder function without compromising sexual function. Posterior repair is a surgical procedure to repair or reinforce the weakened layers between the rectum and the vagina. The aim of the surgery is to relieve the symptoms of vaginal bulging/ laxity and to improve bowel function, without interfering with sexual function. If the uterus is prolapsing, it may be removed (hysterectomy). If the patient already had a hysterectomy, then the top of the vagina (vault) can be lifted up and supported. Surgeons often carry out more than one of these repairs simultaneously. **Hysterectomy** can be considered a treatment option for women who desire to eliminate any chance of cervical or intrauterine pathology, do not desire to get pregnant, or do not wish to preserve future fertility [41, 56].

Obliterative procedures to manage pelvic organ prolapse refer to methods used to close or alter the vagina is such a way that reduces the prolapse. This procedure is only available to women with extensive prolapse who have tried all other options and are certain they do not want to have sexual intercourse again. For frail women who are unable to undergo more difficult surgery, this procedure can also be a viable choice [57].

A **surgical mesh** is a medical instrument that is used to add extra support to weakened or injured tissue. This device is mostly made of polypropylene and is used in the surgical treatment of POP. A surgical mesh can be implanted to reinforce the weakened vaginal wall. Surgical mesh for the treatment of POP is currently solely used to suspend the top of the vagina to a structure on the sacrum in abdominal procedures (open, traditional laparoscopic, or robotic aided laparoscopic sacrocolpopexy) [58].

The FDA ordered mesh manufacturers to stop selling devices in the United States for transvaginal repair of pelvic organ prolapse in 2019 [59]. This being said, the FDA continues to conclude that the advantages of surgical mesh inserted transvaginally to treat POP do not exceed the hazards, based on a review of the available data. They demonstrate that these devices do not have a reasonable assurance of safety and effectiveness [58, 59].

The most common complications reported through medical device reports (MDRs) for surgical mesh include [58]:

- Mesh erosion through the vagina (also called exposure, extrusion, or protrusion).
- Pain.
- Infection.
- Incontinence.

Computational biomechanics is a powerful tool that comes in handy in the case of the dimensioning and positioning of prosthetic parts in the system or in the case of the simulation of a surgical operation. This additional knowledge helps surgeons decide which approach should be considered for each patient.

2.4 Magnetic Resonance Imaging

When it comes to treatment implications, accuracy of diagnosis is critical. MRI (Magnetic Resonance Imaging) has been frequently used as a pre-operative examination of PFD [6].

Multidimensional datasets or images representative of the spatial distribution of a specific physical quantity measure can be obtained using an MRI scanner. The spatial-spectral or spatio-temporal distributions can be generated as 2D sectioned images with arbitrary orientation, 3D volumetric images, or even 4D images. Another unique feature of this technique is the nature of the signals utilized to create the photographs, as it does not require the usage of particles or radiation to generate the collected signals, unlike previous methods [60].

2.4.1 Physical principles of magnetic resonance imaging

The term "nuclear magnetic resonance" is still used by some. The term "nuclear" isn't the most accurate as it reminds people of radioactivity, and this approach doesn't require ionizing radiation.

The technique is based on three steps: alignment, excitation and radiofrequency detection. Alignment (Figure 2.6.) refers to the magnetic property of nuclei of some atoms, which tend to orient themselves parallel to a magnetic field (B_0) [61].

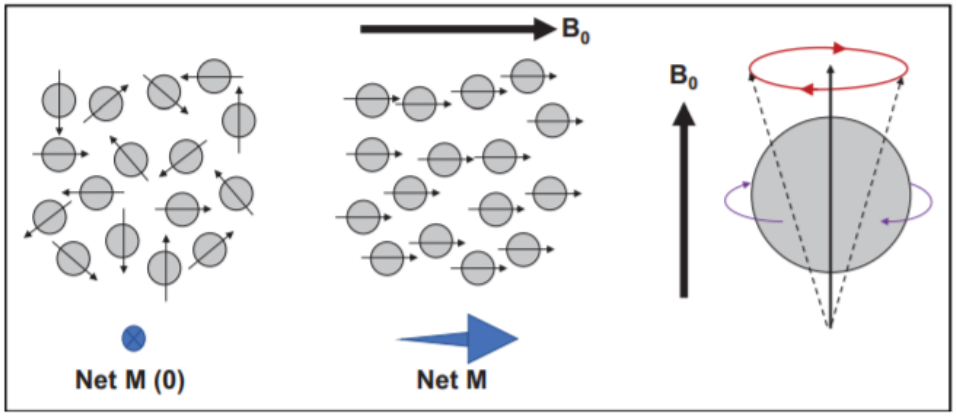

Figure 2.6: Nucleus spin creates polarity with random distribution, producing net magnetic vector (M) of zero (left). Application of strong magnetic field (B_0) creates alignment of proton dipoles, producing net M aligned with B_0 (middle). Although proton dipoles spin on their axis (purple arrows) to produce small magnets, movement in presence of magnetic field is gyromagnetic (red arrows) and termed precession (right) [61].

For physical reasons and because of its abundance, the hydrogen nucleus (proton) is the element used to produce images of biological beings. So, for these atoms to be orientated in a certain direction, an intense magnetic field is required - usually around 1.5 Teslas. Excitation is the following stage. Each hydrogen nucleus is known to "vibrate" at a frequency proportionate to the magnetic field in which it is located. Thus, at 1.5 T, hydrogen has a frequency of 63.8 MHz. The device then emits an electromagnetic wave at that same frequency. There is a transfer

of energy from the wave emitted by the equipment to the hydrogen atoms, a phenomenon known as resonance [62].

Radio frequency detection is the third stage. The energy enabled the hydrogen nuclei to become unstable. At this stage they generate electromagnetic waves at the same frequency when they revert to their normal state (63.8 MHz - radio wave band). Then the equipment detects these waves and determines the position in space and the intensity of the energy. This intensity is shown as "brightness" in the image, and the nomenclature "signal intensity" is used [62].

Depending on how and how long we excite the atoms, the images can be more sensitive to different tissue properties. For example, we have T2-weighted images, in which liquids, demyelination and areas of edema in the brain tissue are clearer - high signal. On T1 images, the white matter is lighter than the grey matter and areas with high protein content and adipose tissue in general have higher signal - clearer [62].

2.4.2 The use of MRI in biomedical sciences

MR images have a greater ability to demonstrate different structures in the brain and can easily demonstrate minimal changes in most diseases. Morphological changes are more easily assessed than on CT, as well as there is greater sensitivity for demyelinating diseases and infiltrating processes. It is also possible to evaluate structures such as the hippocampus , basal nuclei and cerebellum (which is difficult to evaluate on CT) - in some cases necessary for research into mental disorders [62].

The creation of the MRI scan is a defining moment in medical history. Doctors, scientists, and researchers can now use a non-invasive equipment to examine the inside of the human body in great detail. Below are some occasions in which an MRI scanner would be advantageous [63]:

- Anomalies of the brain and spinal cord
- Tumors, cysts, and other anomalies in various parts of the body
- Breast cancer screening for women who face a high risk of breast cancer
- Injuries or abnormalities of the joints, such as the back and knee
- Certain types of heart problems
- Diseases of the liver and other abdominal organs
- The evaluation of pelvic pain in women, with causes including fibroids and endometriosis
- Suspected uterine anomalies in women undergoing evaluation for infertility

This is by no means a complete list. The range and application of MRI technology is constantly expanding.

2.4.3 Magnetic Resonance Imaging of the Pelvic Cavity

In comparison to other imaging modalities such as ultrasound and computed tomography, MRI in gynecology provides more information on the anatomy of the female pelvis. As a result, MRI is the preferred approach for diagnosing and staging gynecologic neoplasms, as well as evaluating therapy response and detecting relapse following treatment. Inconclusive pelvic ultrasound examination, evaluation of surgical sequelae, pelvic pain, vaginal or uterine abnormalities, and PFD are all non-oncologic indications for MRI of the female pelvis [64].

The pelvic floor support structures can be directly visualized via MRI. Patients with multicompartment physical examination findings or symptoms, posterior compartment abnormalities, significant prolapse, or recurrent pelvic floor complaints after past surgical correction may benefit most from using MRI to examine pelvic floor issues. This technique has been proven in several trials to be a valuable tool for detecting and staging POP, with detection rates comparable to fluoroscopic procedures and the ability to identify more extensive organ prolapse than a physical examination alone. [65]

Figure 2.7 shows an example of a sagittal image provided from an MRI exam.

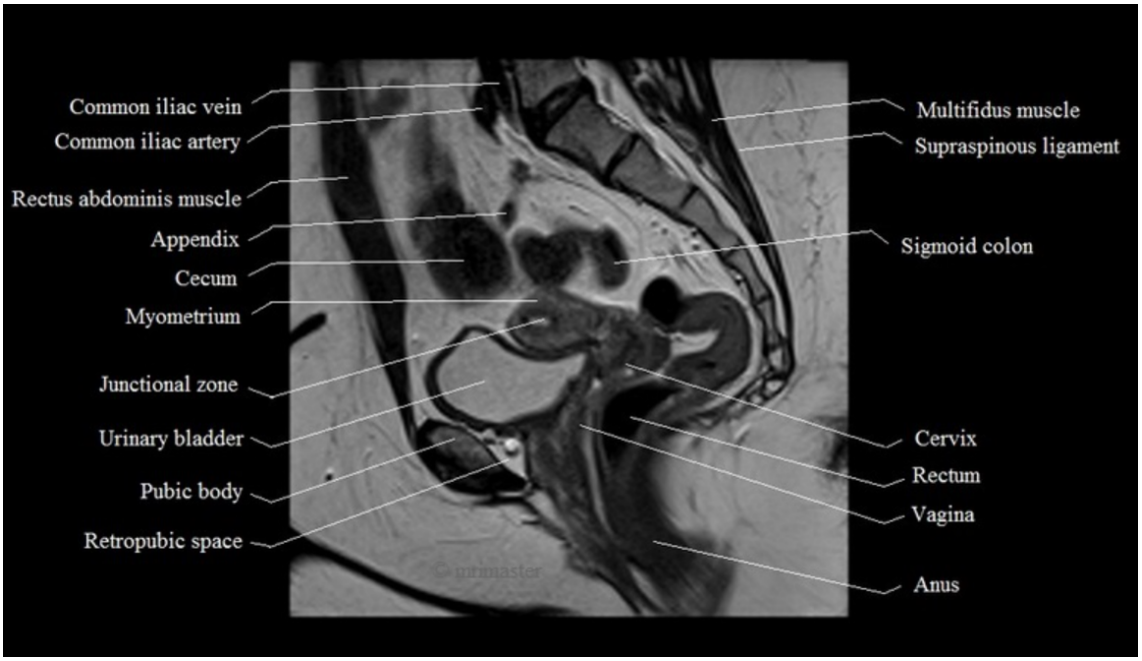

Figure 2.7: Magnetic resonance of the female pelvic cavity acquired at sagittal plane [66].

Chapter 3

Morphing Algorithms for Finite Element Analysis

Nowadays, all but the simplest problems are analyzed and solved with the help of a computer software that speeds up calculations [67]. To study the biomechanical behaviour of anatomical structures the FEM (Finite Element Method) is used.

This method is a numerical technique that aims to determine the structural state of a body, providing approximate solutions to differential equations that model problems that arise in areas such as physics and engineering. This method consists of dividing the domain of the structure under study into smaller areas (finite elements) connected by nodes, thus forming a computational mesh. Once divided into subdomains, it becomes easier to find the desired solutions [67].

The process involved in creating a three-dimensional model can take up to 80 % of the time when it comes to engineering design and the development of CAD models [68]. The development of 3D pelvic models must take into consideration the shape of the structure. The biomechanical response of a system is heavily influenced by its shape. Shape, however, can differ greatly between people or change as a result of aging or disease [69].

The pre-processing setup can be very time-consuming when the FE model is based on real images, particularly in 3D and when the task has to be replicated multiple times for similar applications [70].

The goal of this study is to apply the developed algorithm to a real anatomical structure obtained from real MRI images. For this, there are a great number of techniques to adapt the shape of a geometry, for this study radial basis functions (RBFs) based mesh morphing are used [71].

3.1 Finite Element Method

Modeling physical events is one of the most significant things engineers and scientists study. Almost any natural event—whether aeronautical, biological, chemical, geological, or mechanical can be explained in terms of algebraic, differential, and/or integral equations linking numerous numbers that define the phenomenon, using the laws and axioms of physics or other sciences.

Many key practical challenges that engineers deal with include determining the stress distribution in a great number of anatomical structures, predicting numerous outcomes of clinical situations.

The finite element method is a numerical method that is thought to be particularly powerful in its application to real-world problems including multiphysics, intricate geometry, and boundary conditions [72].

When using this method, a given domain is represented as a collection of subdomains, this numerical technique intends to to solve complex problems, or even problems with no analytical solution, through the sequential and structured resolution of several simpler problems with mathematical solution, which when grouped together, form or lead to a solution of the initial global problem. The main reason behind seeking approximate solutions on a collection of subdomains is the fact that it is easier to represent a complicated function as a collection of simple polynomials [72].

3.1.1 Basic Concepts of the Finite Element Method

The finite element method is essentially a dynamic methodology. It can be used to tackle one-dimensional issues, but it's more commonly used to find a solution in a three-dimensional area or volume. In either of these circumstances, the domain of the system under investigation must be represented, or a more simplified viable representation must be employed. The domain to be examined is divided into a finite number of smaller segments, these finite elements are connected by nodes and together they form a computational mesh. [72]. This task is known as discretization and is visibly portrayed in Figure 3.1.

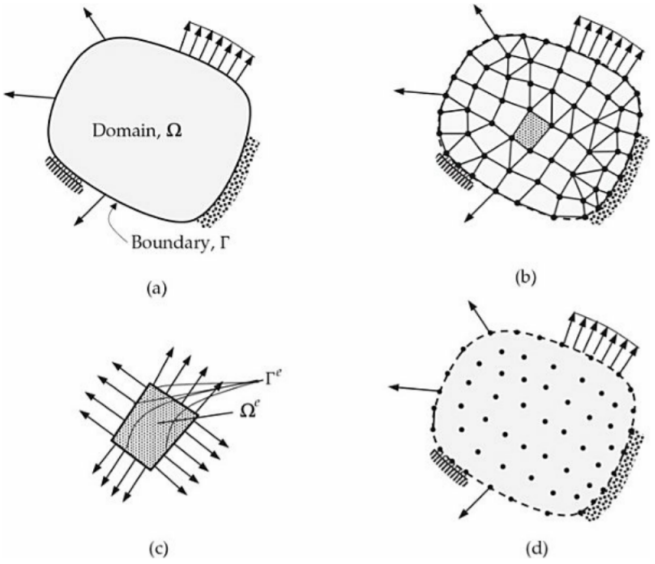

Figure 3.1: Discretization of a two-dimensional domain. (a) Original domain with boundary. (b) Representation of the domain by a collection of triangles and quadrilateral elements. (c) A typical element with domain and boundary. (d) Representation of the domain by a collection of nodes. [72]

The elements' shapes, sizes, numbers, and configurations must be carefully chosen to simulate the original body or domain as precisely as possible without increasing the computational effort required for the solution. The geometry of the body and the number of independent coordinates required to represent the system largely dictates the type of element used. We can employ the one-dimensional or line elements illustrated in Figure 3.2 if the geometry, material properties, and field variable of the problem can be stated in terms of a single spatial coordinate [73].

Figure 3.2: One-dimensional element [73].

The two dimensional elements depicted in Figure 3.3 can be used when the configuration and other characteristics of the problem can be stated in terms of two independent spatial coordinates. The triangle element is the most fundamental element for two-dimensional analysis. Although a quadrilateral element (or its special forms, the rectangle and parallelogram) can be created by joining two or four triangle elements, as shown in Figure 3.4, there are times when using quadrilateral (or rectangle or parallelogram) elements is desirable [73].

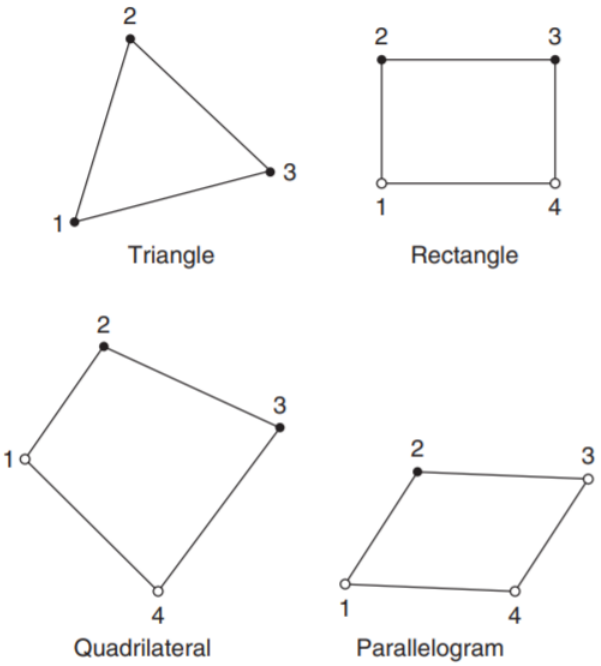

Figure 3.3: Two-dimensional elements [73].

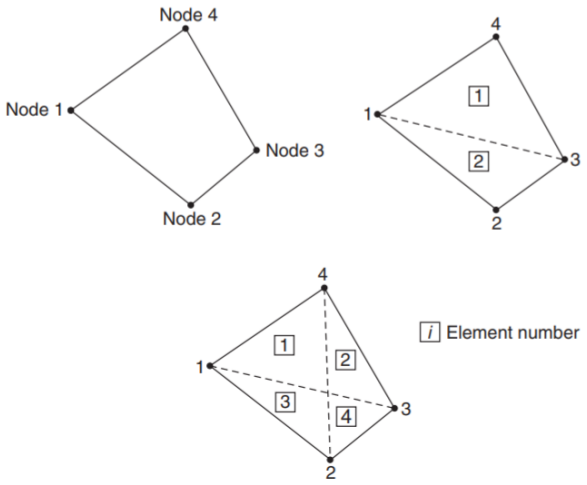

Figure 3.4: A quadrilateral element as an assemblage of two or four triangular elements. [73].

We can idealize the body using the three-dimensional elements presented in Figure 3.5 if the geometry, material characteristics, and other parameters of the body can be specified by three independent spatial coordinates. The tetrahedron is the basic three-dimensional element, comparable to the triangle element in two-dimensional problems. The hexahedron element, which may be made by combining five tetrahedrons, can be useful in particular situations [73].

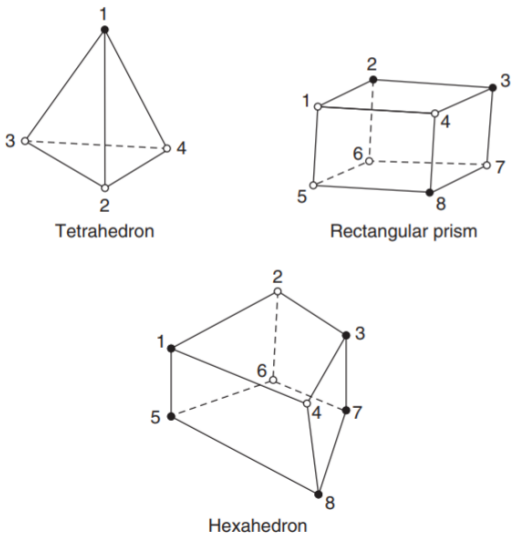

Figure 3.5: Three-dimensional finite elements. [73].

The finite element approach works by treating a body as a collection of elements (or subdivisions) that are connected at specified node positions. Inside any finite element, the unknown solution or field variable (e.g., displacement, pressure, or temperature) is assumed to be given by a

simple function expressed in terms of the nodal values of that element. When developing the system or overall equations, the nodal values of the solution, also known as nodal degrees of freedom, are handled as unknowns. The values of the unknown nodal degrees of freedom are determined by solving the system equations. One will know the solution within any finite element once the nodal degrees of freedom are determined [73].

3.1.2 A General Procedure for Finite Element Analysis

The general procedure for a finite element analysis (FEA) can be summarised in a set of steps, these are:

Table 3.1: Traditional steps for a FEA [74]

Step	Definition
1	Discretization of the structure. The continuous system (geometry) is subdivided into finite elements, generating this way a finite element mesh.
2	The elements are connected by a discrete number of nodal points located at their boundaries; called nodes.
3	Definition of the material properties of the elements.
4	Choosing a set of functions to define the displacement state within each "finite element" in terms of its nodal displacements.
5	Displacement functions define the state of deformation within an element in terms of the nodal displacements. These strains together with the initial strains and the constitutive properties of the material define the stress state across the elements.
6	Establishment of the stiffness matrix, which is derived from a method based on shape functions. This matrix relates the nodal displacement, velocity and acceleration in the forces applied on the nodes.
7	Load application - forces or moments are applied externally in a concentrated way or a distributed way.
8	Definition of boundary conditions.
9	Solving systems of linear algebraic equations.
10	Calculation of displacement, stresses, reactions or other post-processing information.

There are three stages for numerical simulation using the finite element method: 1) pre-processing; 2) analysis; and, 3) post-processing.

The pre-processing stage concerns the construction of the geometric model of the system to be studied and the definition of the loads and conditions to which it will be subjected. The global quality of an analysis using the finite element method depends, to a large extent, on the way the user approaches this pre-processing phase, including possible simplifications to be considered in the modeling and in the choice of the type of elements and mesh to be used. It is also in this first phase that all the mechanical and/or physical properties of the materials to be used in the model are defined. Finally, all the loads and constraints to which the model may be subjected are defined. These restrictions are often called boundary conditions [75, 74].

The post-processing phase takes care of the task of presenting the information contained in the result output files.

Figure 3.6 presents a representation of the typical analysis methodology of a problem using FEM.

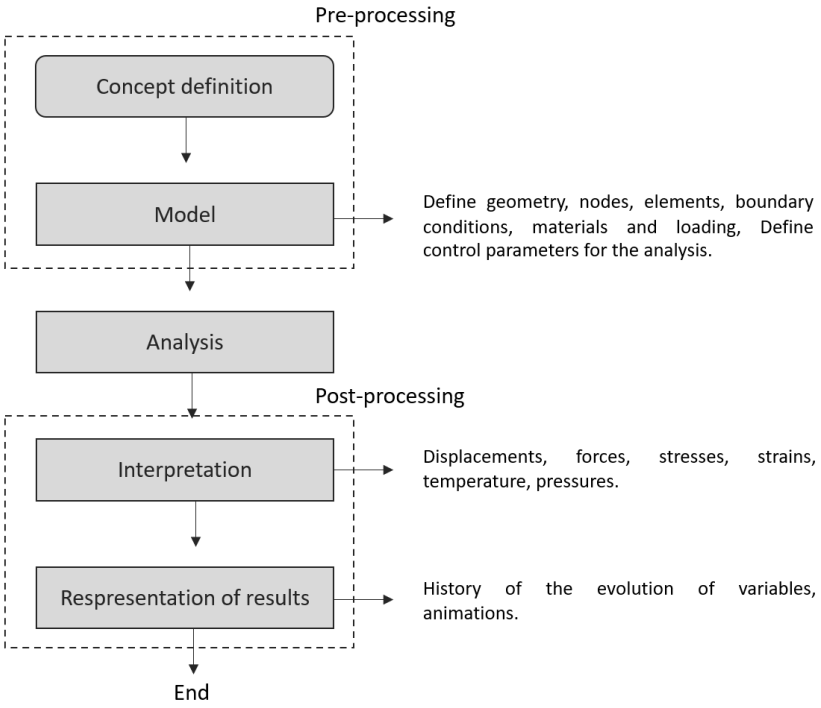

Figure 3.6: Finite Element Method representation.

3.2 Mesh Morphing Algorithms

Meshes have become a common and widely used model representation in computer graphics. The goal of morphing techniques is to change a given source shape into a target shape. Morphing techniques are used in a variety of settings, from television and film special effects to medical imaging and scientific visualization.

Many iterations of geometric design changes are often included in the modeling and simulation process. An optimization approach is used to drive geometric parameters automatically. To enable rapid prototyping of many different geometric designs, the ability to instantly update an existing mesh to adhere to a changing geometry is a necessary capability. Mesh morphing, mesh warping, and mesh shifting are terms used in the literature to describe this mesh updating process. To conform to geometry changes, these techniques first maintain a stable mesh topology while computing new positions for mesh nodes [76].

There are a great number of techniques to adapt the shape of a geometry, for this study radial basis functions (RBFs) based mesh morphing was used. This method works by adapting the

geometry's shape based on the update of its nodes positions [71]. This free mesh connection approach can mesh fluid or solid domains and can handle both structured and unstructured grids.

3.2.1 Radial Basis Functions Mesh Morphing

Hardy [77] established radial basis functions (RBF) in the late 1960s as a powerful mathematical tool for interpolating scattered data in the field of surveying and mapping.

RBF is now widely used in a variety of engineering applications and is widely regarded as one of the most powerful and versatile mathematical approaches for mesh morphing management. In the case of 3D mesh morphing, a vector field is defined by independently interpolating the three components of the displacement known at source locations. The RBF vector field is a point function that exists independently of the mesh; any points in the space that receive the field are referred to as targets. A typical mesh morphing problem that can be faced using RBF consists in a three-dimensional mesh to be adapted according to a known displacement of the surface; surface nodes are extracted from the surface mesh as sources and all the nodes of the volume mesh receive the morphing field as targets [78, 79].

Mesh morphing is of great importance when it comes to individually mesh a great number of geometries with shape variations [68]. With the implementation of this technique, the CAE grid is updated onto a new design. Instead of producing a new mesh for the modified geometry, the original mesh is updated onto the new configuration.

When using RBF morphing techniques, the three displacement field's components are assigned to the control cloud points. These points are commonly referred to as source points, and they are interpolated in space to update the nodal coordinates of the mesh to be morphed [71].

The coefficients of a linear system of order equal to the number of control points are calculated in an RBF problem, allowing the displacement of an arbitrary mesh's node (target) to be represented, and then imposed, as the total of the radial contributions of each controlled node (source). Mesh smoothing can be applied quickly while still retaining mesh topology in terms of total number and kind of elements [80].

Equations 3.1 and 3.2 show the mathematical phenomenon explained previously.

$$\begin{cases} u(x) = \sum_{i=1}^{N} \gamma_i^u \varphi\left(\|x - x_{s_i}\|\right) \\ v(x) = \sum_{i=1}^{N} \gamma_i^v \varphi\left(\|x - x_{s_i}\|\right) \\ w(x) = \sum_{i=1}^{N} \gamma_i^w \varphi\left(\|x - x_{s_i}\|\right) \end{cases} \tag{3.1}$$

Mesh deformation based on RBF is a node-by-node method that does not rely on mesh connectivity. It propagates the known motion of a cloud of control points to the mesh nodes using interpolation [81]. When the displacement field is applied all the nodal positions are updated, generating a new set of points.

$$x_{\text{node-updated}} = x_{\text{node}} + \begin{bmatrix} u\left(x_{\text{node}}\right) \\ v\left(x_{\text{node}}\right) \\ w\left(x_{\text{node}}\right) \end{bmatrix} \tag{3.2}$$

The local deformation due to the morphing field can be inspected by computing the derivatives of the three components of displacement thus obtaining the strains as follows:

$$\varepsilon_x = \frac{\partial u}{\partial x} \varepsilon_y = \frac{\partial v}{\partial y} \varepsilon_z = \frac{\partial w}{\partial z} \varepsilon_{xy} = \frac{\partial u}{\partial y} + \frac{\partial v}{\partial x} \varepsilon_{yz} = \frac{\partial v}{\partial z} + \frac{\partial w}{\partial y} \varepsilon_{xz} = \frac{\partial u}{\partial z} + \frac{\partial w}{\partial x} \tag{3.3}$$

In this field mesh morphing can be used as a tool for shape registration that consists in deforming a template geometry onto a target one, that is, adapting a template mesh onto a subject-specific geometry extracted from magnetic resonance images.

3.2.2 Application of Morphing Algorithms in Computational Biomechanics

Mesh morphing is of great importance when it comes to individually mesh a great number of geometries with shape variations [68]. With the implementation of this technique, the CAE grid is updated onto a new design. Instead of producing a new mesh for the modified geometry, the original mesh is updated onto the new configuration.

There are a great number of techniques to adapt the shape of a geometry, for this study radial basis functions (RBFs) based mesh morphing was used. This method works by adapting the geometry's shape based on the update of its nodes positions [71]. This free mesh connection approach can mesh fluid or solid domains and can handle both structured and unstructured grids.

With the use of computational modeling it becomes possible to simulate various clinical outcomes by developing specific models that reproduce the mechanical and geometric characteristics of an anatomical region of interest from biomedical images, intended for diagnostic, therapeutic, or surgical purposes. When they are sufficiently reliable, these models can represent a virtual patient, thus being able to replace human clinical evaluation in some situations.

Figure 3.7 and 3.8 summarizes the work flow of a typical mesh morph procedure.

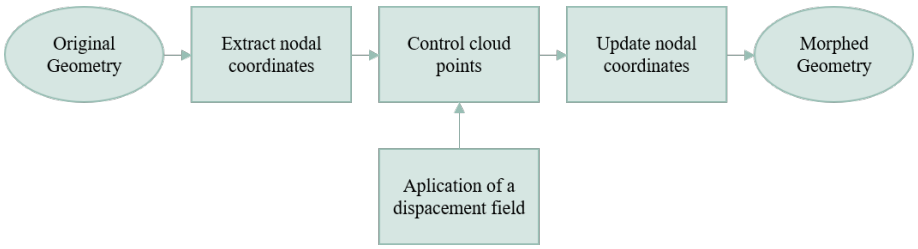

Figure 3.7: General pipeline of a mesh morphing procedure.

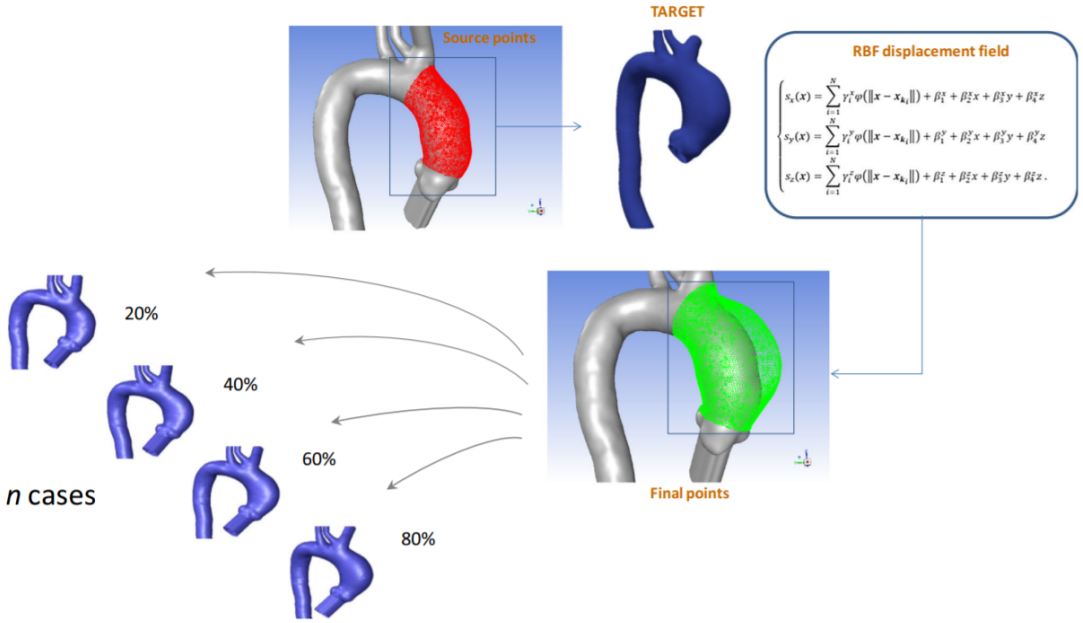

Figure 3.8: Graphical representation of a mesh morphing based workflow, adapted from [82].

The last image displays how the geometry of an average healthy patient can be evolved onto the aneurysm affected one.

Chapter 4

Methodology

This chapter focuses on the presentation of some preliminary work during the course 'Trabalhos Práticos. This consists in an introduction to the software used for the application of morphing algorithms to a less complex structure.

Furthermore, in this chapter the methodology followed to obtain the results needed for the present dissertation is discussed.

4.1 Preliminary Work

To develop the algorithms required for this project MATLAB was the software of choice. MATLAB is considered a high-level language that was created specifically for working with matrices, making it ideal for programming the finite element method.

Firsty, an STL file was exported from Abaqus with all the information needed. This openly documented format is commonly used to describe the surface of a 3D geometry as a triangular mesh, by representing a three-dimensional surface in triangular facets.

Once imported to MATLAB, the geometry developed was used to extract the nodal coordinates required to adapt the structure. A matrix of points was then defined with the purpose of conceiving the desired control cloud point. As a consequence of the way the STL format works the formerly hexahedral elements had to be transformed into triangular elements. This resulted in a loss of accuracy, changing the number of nodes from 891 to 450. All 450 nodes are displayed in Fig. 4.1, for a better visualization, a triangular meshed was applied to the original geometry.

For the nodal positions to be updated a displacement of 0.5 units in the x-axis was applied to each node. This resulted in a longitudinal length increase of 5 units.

The results obtained by the implementation of a morphing procedure to a pre-existent mesh resulting in a new geometry are displayed in Figure 4.2

The mesh morphing action was accomplished using a set of MATLAB functions. A set of source points was selected to generate a shape variation representative of the desired displacement.

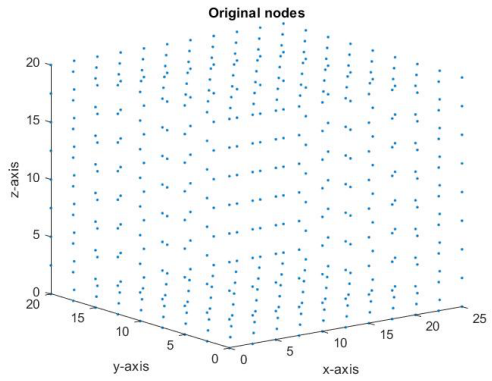

(a)

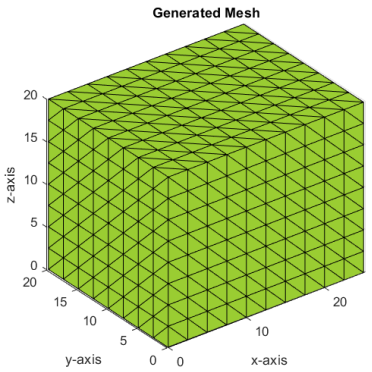

(b)

Figure 4.1: a) Cloud of control points obtained from the developed geometry. and b) Obtained mesh.

To achieve this, the displacement was applied to each pre-existing node excluding the ones that belong to the geometry's left side, causing it to become motionless, resulting in an updated location of the set of control points.

With this new set of points a new computational mesh was generated which was ready to be exported in STL format for future analysis.

When comparing Figures 4.1 and 4.2 it can be noted an increase in the length of the structure by 5 units (the structure goes from a 25 to a 30 unit length).

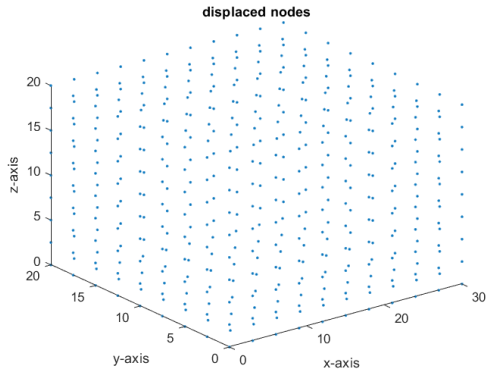

(a)

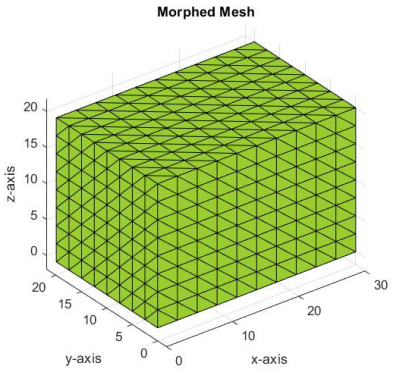

(b)

Figure 4.2: a) Cloud of control points obtained from the developed geometry. and b) Obtained mesh.

The RBF method showed its suitability for the proposed application due to the fact that they use points to specify features in the structures, and these points have no restrictions on their location on the geometry. As a result, the radial basis functions showed an easily controllable behavior since there are no restrictions on the positions of the control points on the geometries.

In order to take this study to another level, real MRI images from pelvic structures are taken into account. For the proposed work a morphing procedure will be applied to a female pelvic bone (Figure 4.3).

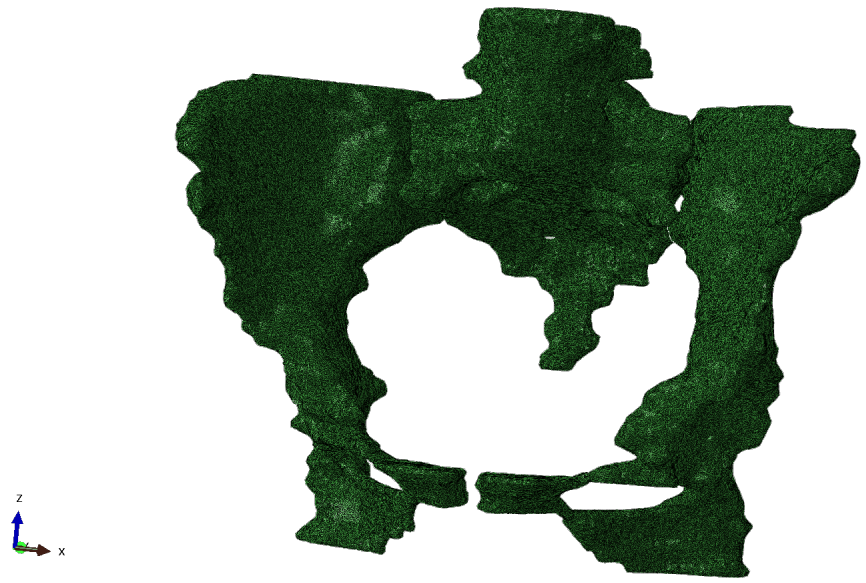

Figure 4.3: Three-dimensional model of the female pelvis.

4.2 Computational Model of the Female Pelvic Bone

The model presented previously is a result of image segmentation, a tool that allows regions of interest (ROIs) to be extracted from 3D image data. The major objective of segmenting this data is to identify the anatomical regions needed for a given study, such as simulating physical properties or realistically putting implants with CAD designs inside of patients [83].

Similar to what was done before in the preliminary work, the CAD model was imported into Abaqus and a computational mesh was applied to it, the geometry was composed of:

- 1309031 linear tetrahedron elements of type C3D4H;
- 363250 nodes.

This model belongs to an asymptomatic 35-year-old woman and was obtained using a semi-automatic process, via the Mimics Innovation Suite v. 17 software.

In contrast to the procedure followed before, the model was not exported as a .stl file but as an .inp file. This choice was made because INP files are the input files utilized by the Abaqus engineering simulation and analysis program, they are classified as data files. They provide a more accurate information about spacial distribution of nodes and elements.

Once all the information needed is extracted, the analysis and morphing procedure can take place. For that, MATLAB is utilized once again.

4.3 MATLAB Implementation

When imported to MATLAB, the .inp file showed overlapping in nodal coordinates and their corresponding elements. To tackle this issue, the main file had to be separated into several files, one for each structure. A script was then produced in order to renumber the nodes' and elements' ids so that no conflicts are presented when the morphing procedure starts.

After this, all the files are loaded into MATLAB and all the nodal coordinates and elements are concatenated into two different matrices. For a better visualization, Figure 4.4 shows a plot with all the structure's nodes.

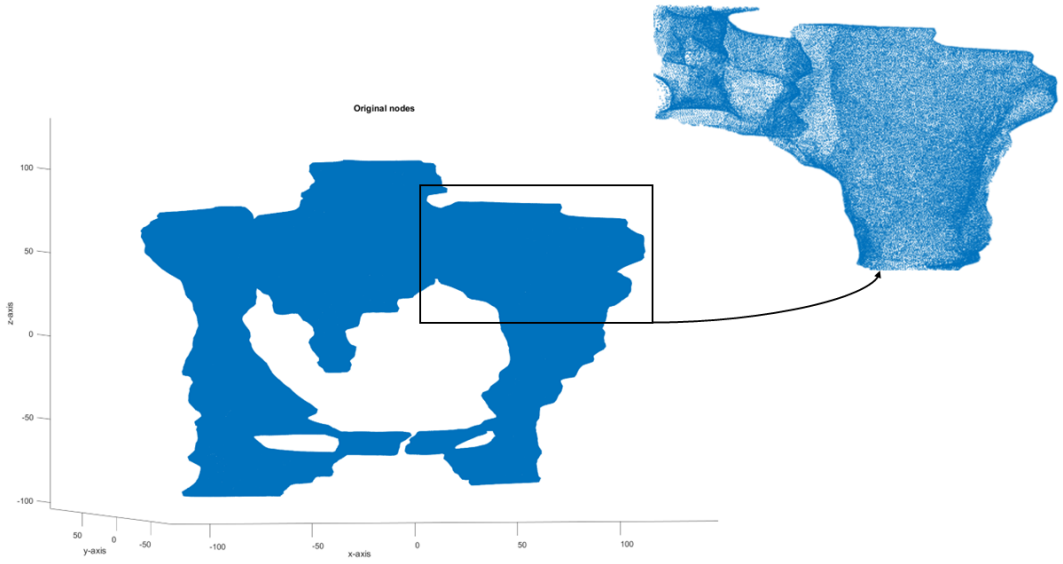

Figure 4.4: Original nodal coordinates for the proposed model.

The next step to consider is the implementation of boundary conditions to the geometry. In computational mechanics, boundary conditions are both realistically necessary for specifying a problem and of crucial relevance. The need for the complex computational study of systems with shifting boundaries has grown in recent years. Particle simulation technologies have drawn increasing interest as a new potential computing paradigm in a variety of scientific and engineering domains. One of its key characteristics is a high flexibility in simulating boundaries with violent motion [84].

In order to set the needed boundary conditions, a set of nodes was chosen in Abaqus through the query tool. These nodes refer to the sacrum, this structure is chosen due to its relative position, acting as a middle-ground for the computation procedure. The structure becomes stationary, This

means that the displacement in any direction will be zero. If there are rotational degrees of freedom, these will also be zero. This proves to be helpful when applying a displacement field to the original geometry.

Figure 4.5 shows, with red circles, the points chosen to accomplish what was previously mentioned.

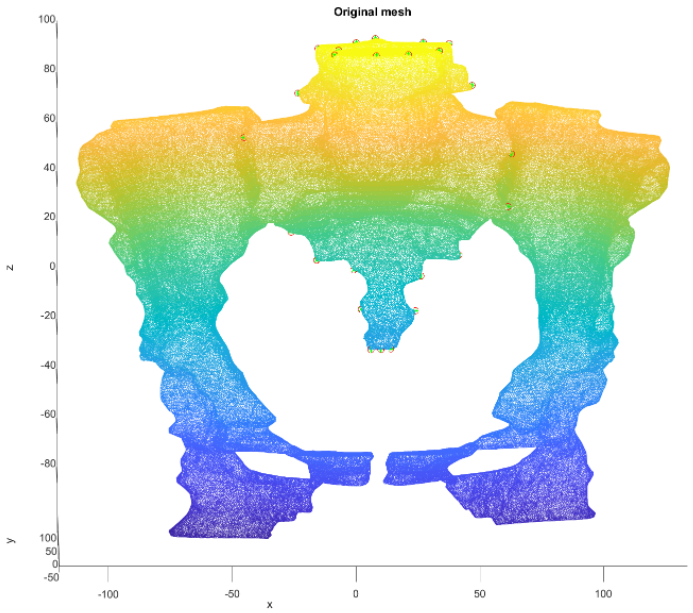

Figure 4.5: Original mesh with the needed fixed nodes.

The decision for which landmarks to choose to adapt came from the revision of pelvimetry. Using clinical examination, standard X-rays, computerized tomography scanning, or magnetic resonance imaging, this procedure aims at the measurement of the size of a woman's pelvis. The most commonly used measurements are those that refer to the the midpelvis, the outlet, and the inlet (the obstetric conjugate) [85].

These landmarks are defined by:

- **Pelvic inlet**: Obstetrical conjugate refers to the line that runs between the sacral promontory and the inner pubic arch, which are the two narrowest bony points: It has to be 11.5 cm or longer. Compared to the diagonal conjugate, this anteroposterior line at the inlet is 2 cm shorter (distance from undersurface of pubic arch to sacral promontory). The pelvic inlet's transverse diameter is 13.5 cm;

- **Midpelvis**: The ischial spines are connected by a line that, on average, is wider than 12 cm between the thinnest bone points;

- **Pelvic outlet**: The distance between the ischial tuberosities (typically > 10 cm).

It's important to note that these measurements (Fig. 4.6) vary between different women, thus the importance of a mesh morphing procedure, to develop a personalized study taking into account each individuals landmark's distances.

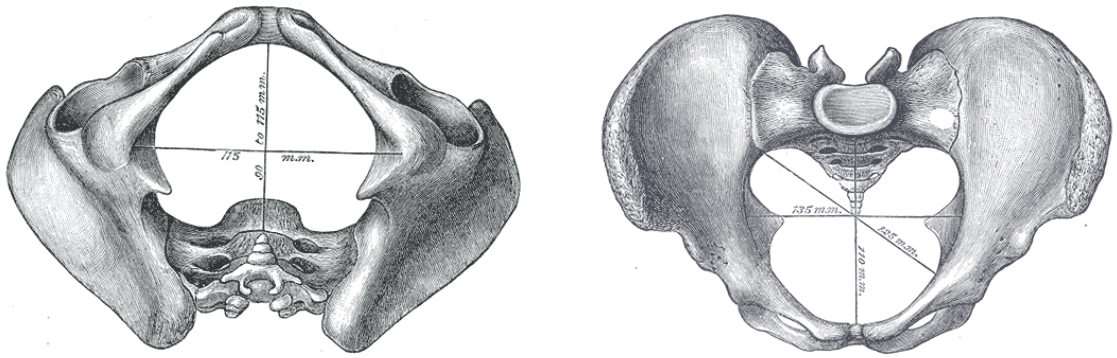

(a) (b)

Figure 4.6: Diameters of inferior aperture of lesser pelvis [9] a) Inferior view and b) Superior view

As an arbitrary example, some nodal coordinates were chosen through the query tool on the Abaqus software. The nodes selected to update the geometry correspond to the iliac crest and iliac spine as one can observe in 4.7. To change the shape of the model a new distance is defined between the selected points, which are highlighted with a green dot. A new length is computed in MATLAB and the new positions appear in a new set of red circles.

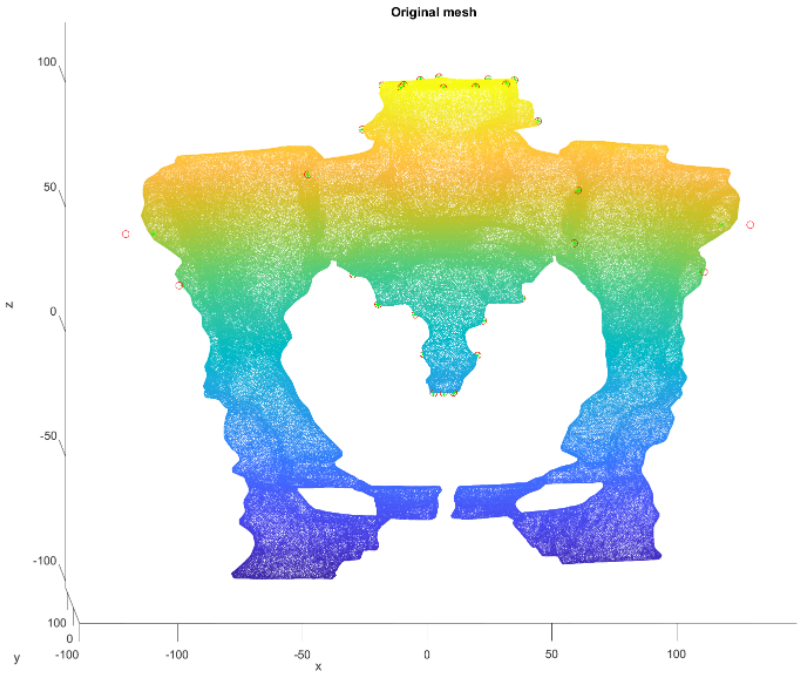

Figure 4.7: Original mesh with the selected landmarks.

In the following chapter the results obtained through the computational morphing procedure are presented.

Chapter 5

Results and Discussion

One of the simplest mesh morphing paradigms, the RBF, is considered to be one the one of the easiest to automate, it uses all of the nodes (or a subset of them) on the surfaces as sources coordinates [71]. The study that is described here is based on such an approach for the purpose of simplicity. The illustration in Fig. 5.1 shows how the distance between the iliac crests and spines can be used to update the mesh of the ilium.

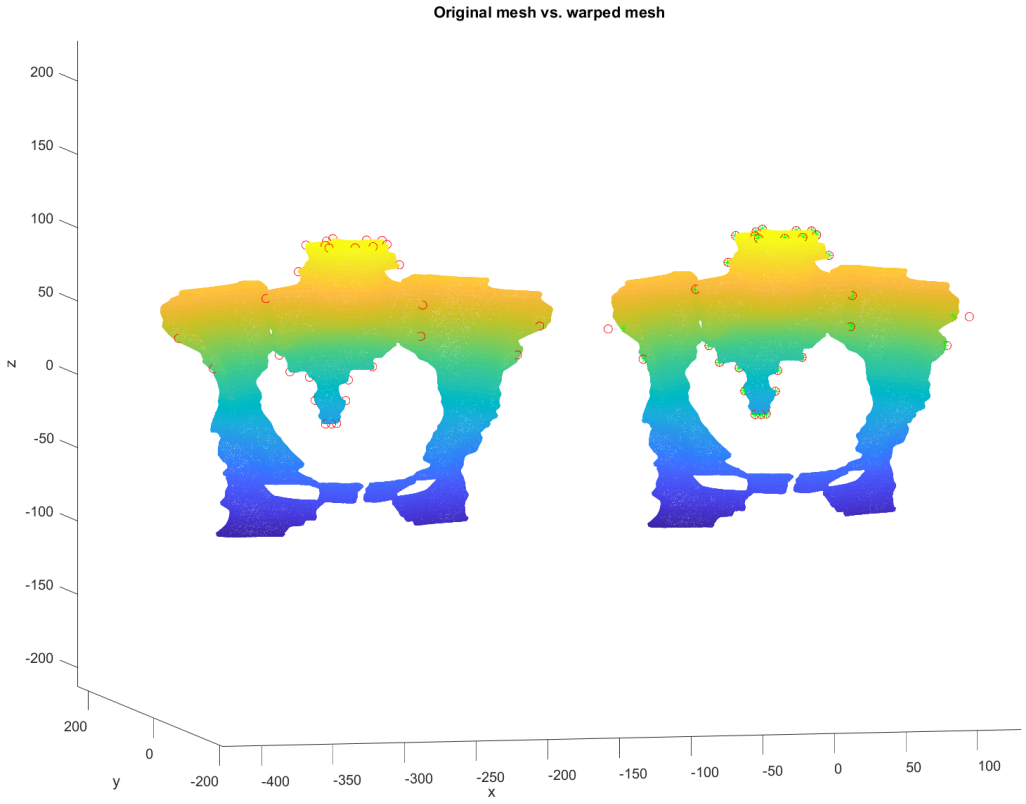

Figure 5.1: Original mesh and wrapped with the selected landmarks.

In order to take this study to another level most of the organs present in the pelvic cavity needed to be taken into consideration. Since the purpose of this study was to create new models to be used in a pelvic surgery simulation setting, all the structures illustrated in Figure 5.2 were added onto the model's configuration.

Another goal is the morphing of the soft pelvic structures, whose target is to reduce the time in building the model from the medical images. Later these techniques will allow a faster adaptation of the model to a specific case, such as a patient who will undergo surgery.

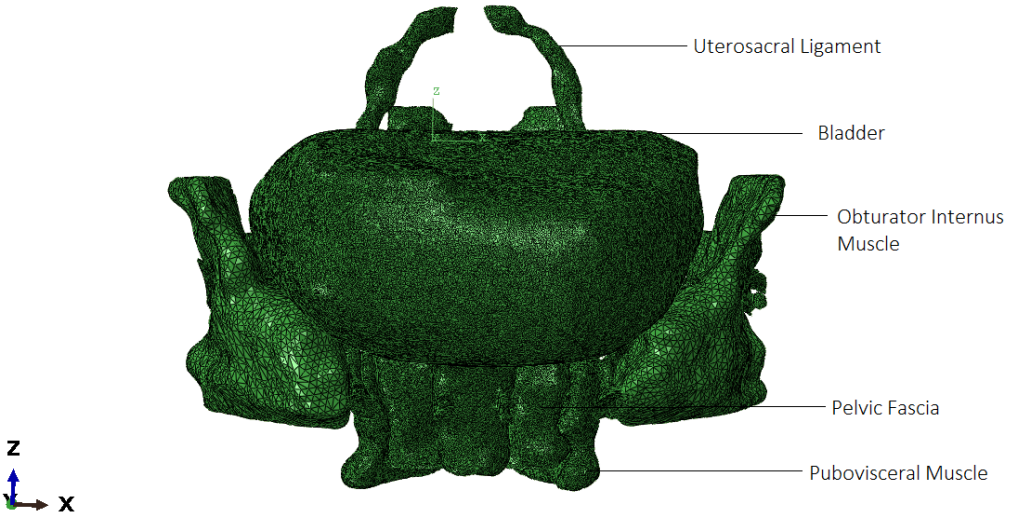

(a)

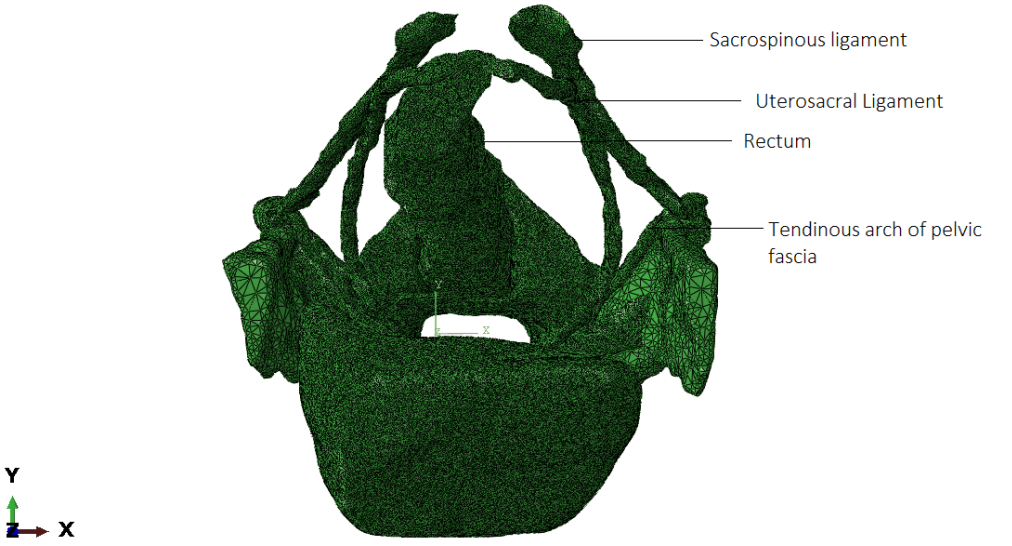

(b)

Figure 5.2: Additional Structures added onto the model a) Front view and b) Top view.

The complete model can be seen in Figure 5.3, this geometry is composed of:

- 2176075 linear tetrahedral elements of type C3D4H;
- 618501 nodes.

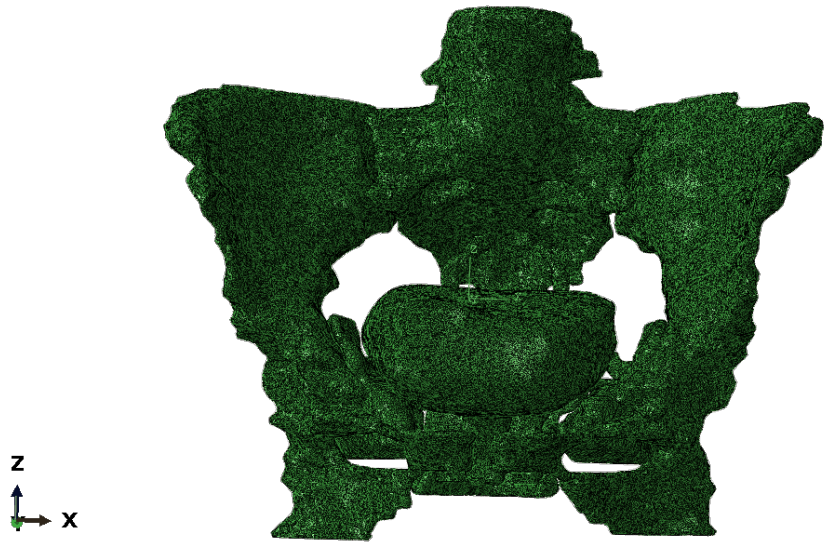

Figure 5.3: Original model with all the added structures.

Both technical and cognitive mistakes can happen to a surgeon regardless of their expertise, such mistakes can result in surgical errors. As their surgical careers take off, with less experience and training, resident surgeons are more likely to make surgical mistakes. An innovative technique that can identify, characterize, and explain surgical mistakes utilizes biomechanical motion analysis and a high-fidelity 3D surgery simulator has been developed in order to quantify surgical errors and speed up the learning process for surgeons.

In vaginal mesh surgery, a plastic structure that resembles a net and is made of synthetic material is implanted to hold the pelvic organs in place. It would be of great interest to produce meshes that take into consideration the shape and size of each individual's organs.

Figure 5.4 depicts how the shape of an anatomical geometry can be updated when certain landmarks are selected and new distances are computed.

As the interspinous distance and the transversal diameter were increased, a wider shaped pelvis was obtained. This shape of pelvis is consistent with a gynaecoid pelvis. The small structural variations between both models result in a larger pelvic inlet (left model presented in Fig. 5.4), which is designed to facilitate birthing. In contrast to the other, the gynaecoid pelvis has:

- A wider and broader structure;
- An oval-shaped inlet when compared with the android pelvis.

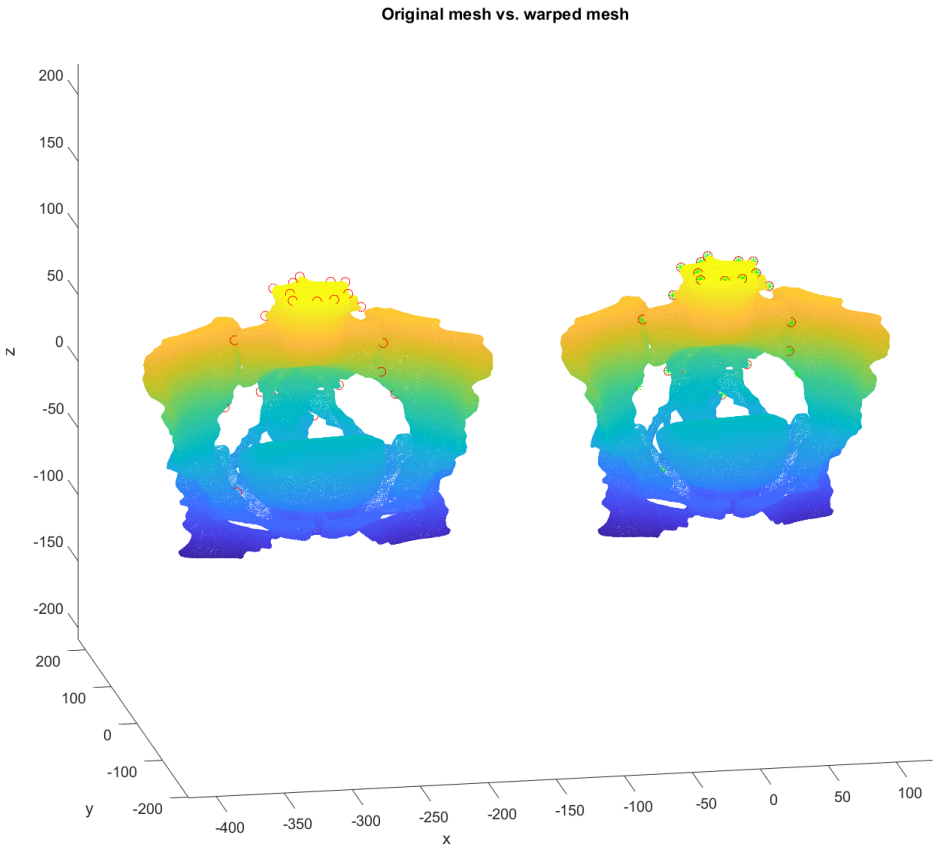

Figure 5.4: Obtained results from the morphing procedure- increase in the interspinous distance and transverse diameter.

Once the morphing procedure is completed the nodal coordinates of the original set of points is updated and new input file is created. This new file was then imported into Abaqus (Figure 5.5 and 5.6) and it was ready to be used in simulations.

Through the query tool new distances were measured, making it possible to confirm that the produced algorithm also worked for the surrounding structures of the pelvic bone. With the increase of the pelvis' width, organs like the urinary bladder are also elongated to accommodate for the transformation.

Mesh independence and node-wise accuracy seem to be two standout benefits of RBF mesh morphing that make it exceedingly versatile. Due to the mesh deformation being a point function after the RBF field is created, nodal locations are updated regardless of the associated mesh components, and interfaces are meshless [86].

The computational procedure was relatively quick, thus proving the superiority of this technique. Instead of recreating a new model from every single patient's medical images it is faster to update a pre-existing geometry. This ends up saving not only computational time but resources.

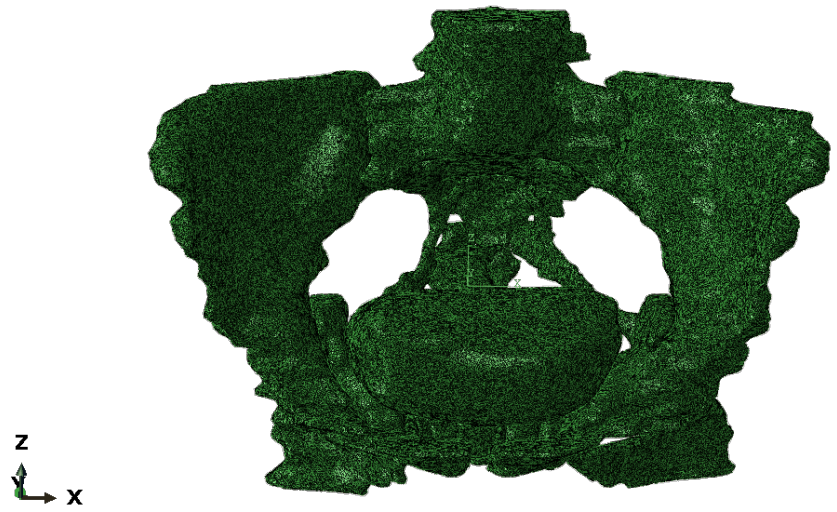

Figure 5.5: Updated geometry obtained through the morphing procedure.

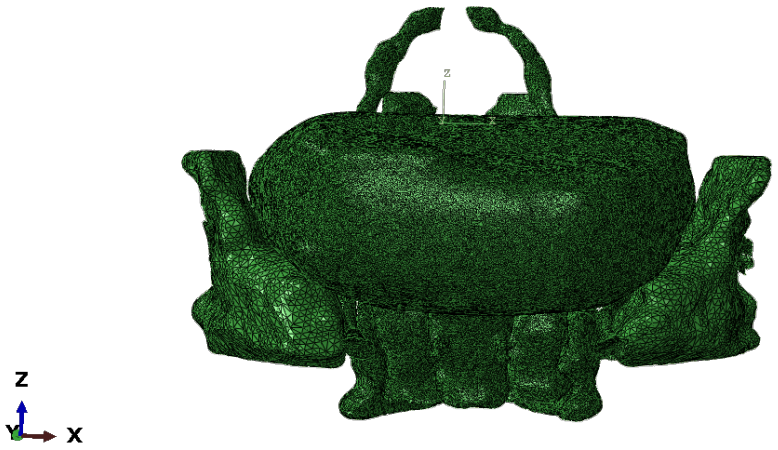

Figure 5.6: Morphed structures.

Chapter 6

Conclusion and Future Work

Pelvic organ prolapse is a condition that can go by unnoticed since the diagnosis is mainly made by visually interpretation of a doctor which can be subjective and misleading. Three-dimensional models come in hand when it comes to aid the diagnostic procedure. These models can be obtained trough medical images but generating a model for each patient is very time consuming.

Mesh morphing is used to reduce the computational process behind the model generation. Instead of producing a new model from scratch, an original geometry is updated through the use of fixed landmarks. The structure changes shape according to the variation of its landmarks.

Usually mesh morphing is faster than remeshing for a number of reasons: it avoids "remeshing noise" (having the same mesh adapted means the effect of a parameter is not confused with the effect of a new mesh structure), so variation effects can be assessed even with a coarser mesh. The CAE model can be updated on the background keeping all the original settings (boundary conditions). The update of nodal positions usually requires less computational efforts vs a full mesh regeneration. Creating shape parameters with mesh morphing is faster than creating a parametric CAD model.

To simplify this study a cubic geometry was firstly used in order to prove the techniques' suitability. In spite of the simplicity of the produced study, it was possible to demonstrate how the RBF techniques operate. As expected the creation of this new model was significantly faster when comparing to a model made from scratch.

Afterwards, the real model was imported to MATLAB, a study of important landmarks was conducted to decide which nodes to be selected from the computational mesh. The distance between them was increased and a new geometry was successfully produced. Once all the needed algorithms were developed the time needed to compute a new model was shorter.

This tool can be very useful to surgeons when practicing for surgery, mistakes can be avoided, and the biomechanical behaviour of the model can be simulated.

Although satisfactory results were obtained, there are some considerations to be taken into account regarding this project. As future work, a more automatic selection of landmarks should be implemented, since selection by node can be misleading and lead to the production of an anatomically incorrect model.

The whole geometry should be meshed as one in order to prevent node and element overlapping and to facilitate the upload of the model onto the computational software.

References

[1] Ian Milsom and Maria Gyhagen. *The Epidemiology, Natural History and Prevention of Pelvic Floor Disorders*. Glob. libr. women's med, 2014.

[2] James A. Ashton-Miller and John O.L. DeLancey. On the biomechanics of vaginal birth and common sequelae. *Annual Review of Biomedical Engineering*, 11(1):163–176, August 2009.

[3] Saori Morino, Mika Ishihara, Fumiko Umezaki, Hiroko Hatanaka, Mamoru Yamashita, and Tomoki Aoyama. Pelvic alignment changes during the perinatal period. *PLOS ONE*, 14(10):e0223776, October 2019.

[4] Ian A. Sigal, Hongli Yang, Michael D. Roberts, and J. Crawford Downs. Morphing methods to parameterize specimen-specific finite element model geometries. *Journal of Biomechanics*, 43(2):254–262, January 2010.

[5] Nathan Lauzeral, Domenico Borzacchiello, Michael Kugler, Daniel George, Yves Rémond, Alexandre Hostettler, and Francisco Chinesta. Shape parametrization of bio-mechanical finite element models based on medical images. *Computer Methods in Biomechanics and Biomedical Engineering: Imaging & Visualization*, 7(5-6):480–489, March 2018.

[6] Shruti Gupta, J. B. Sharma, Smriti Hari, Sunesh Kumar, K. K. Roy, and Neeta Singh. Study of dynamic magnetic resonance imaging in diagnosis of pelvic organ prolapse. *Archives of Gynecology and Obstetrics*, 286(4):953–958, June 2012.

[7] Kiran Gangadhar, Abhishek Mahajan, Nilesh Sable, and Puneet Bhargava. Magnetic resonance imaging of pelvic masses: A compartmental approach. *Seminars in Ultrasound, CT and MRI*, 38(3):213–230, June 2017.

[8] Niaam Khalid, Al-Hayali, Jumaa Chiad, Somer Nacy, and Omar Hussein. A review of passive and quasi-passive lower limb exoskeletons for gait rehabilitation. *Journal of Mechanical Engineering Research and Developments*, 44:436–447, 10 2021.

[9] Susan Standring. *Gray's anatomy : the anatomical basis of clinical practice*. Elsevier, New York, 2021.

[10] Michael G. Funaro and Sonia Bahlani. Anatomy of the female pelvis. In Farzeen Firoozi, editor, *Female Pelvic Surgery*, pages 1–20, Cham, 2020. Springer International Publishing.

[11] MICHELLE K. ROACH and ROCHELLE F. ANDREOTTI. The normal female pelvis. *Clinical Obstetrics & Gynecology*, 60(1):3–10, March 2017.

[12] Frank H. Netter MD. *Atlas of Human Anatomy (Netter Basic Science)*. Elsevier, mar 2018.

[13] Erich Brenner. Anatomy of the upper and lower urinary tract. In *Neurourology*, pages 3–15. Springer Netherlands, 2019.

[14] Junyang Jung, Hyo Kwang Ahn, and Youngbuhm Huh. Clinical and functional anatomy of the urethral sphincter. *International Neurourology Journal*, 16(3):102, 2012.

[15] Marian Stanisław Migda, Michał Migda, Rafał Słapa, Robert Krzysztof Mlosek, and Bartosz Migda. The use of high-frequency ultrasonography in the assessment of selected female reproductive structures: the vulva, vagina and cervix. *Journal of Ultrasonography*, 19(79):261–268, December 2019.

[16] Florence Zara and Olivier Dupuis. Uterus – biomechanical modeling of uterus. application to a childbirth simulation. *Biomechanics of Living Organs: Hyperelastic Constitutive Laws for Finite Element Modeling*, pages 325–346, April 2017.

[17] Brittany Hoare and Yusuf Khan. Anatomy, abdomen and pelvis, female internal genitals. *StatPearls Publishing*, 07 2020.

[18] José Marcio Neves Jorge and A Habr-gama. Anatomy and embryology of the colon, rectum, and anus. In *The ASCRS Textbook of Colon and Rectal Surgery*, 2014.

[19] Yun Hwa W. Wang and Jeffrey Wiseman. *Anatomy, Abdomen and Pelvis, Rectum*, chapter 4, pages 346–393. StatPearls Publishing, 2022.

[20] Heddwen L Brooks Jason X J Yuan Kim E Barrett, Susan M Barman and William F Ganong. *Ganong's review of medical physiolog*, chapter 6, pages 686–693. McGraw-Hill Education, 2019.

[21] Jeremy M. DeSilva and Karen R. Rosenberg. Anatomy, development, and function of the human pelvis. *The Anatomical Record*, 300(4):628–632, March 2017.

[22] Matthew Burgess. *Anatomy, Bony Pelvis and Lower Limb, Pelvic Bones*, chapter 6, pages 686–693. StatPearls Publishing, 2021.

[23] Kahkashan Jeelani. Anatomy of the pelvis in obstetrics. In *Part 1 MRCOG Revision Notes and Sample SBAs*, pages 18–22. Cambridge University Press, November 2020.

[24] T. Editors of Encyclopaedia Britannica. Pelvis: Anatomy. In *Human Anatomy - Pelvis: Anatomy*, 2022. URL: https://www.britannica.com/science/pelvis.

[25] Jeanelle Uy and Natalie M. Laudicina. Assessing the role of the pelvic canal in supporting the gut in humans. *PLOS ONE*, 16(10):e0258341, October 2021.

[26] Katharina Jundt, Ursula Peschers, and Heribert Kentenich. The investigation and treatment of female pelvic floor dysfunction. *Deutsches Ärzteblatt international*, August 2015.

[27] Varuna Raizada and Ravinder K. Mittal. Pelvic floor anatomy and applied physiology. *Gastroenterology Clinics of North America*, 37(3):493–509, September 2008.

[28] F. Michel, P. Decavel, E. Toussirot, L. Tatu, E. Aleton, G. Monnier, P. Garbuio, and B. Parratte. The piriformis muscle syndrome: An exploration of anatomical context, pathophysiological hypotheses and diagnostic criteria. *Annals of Physical and Rehabilitation Medicine*, 56(4):300–311, May 2013.

[29] Mark S. Cook, Laura Bou-Malham, Mary C. Esparza, and Marianna Alperin. Age-related alterations in female obturator internus muscle. *International Urogynecology Journal*, 28(5):729–734, October 2016.

[30] Marlene M Corton. Anatomy of the pelvis: How the pelvis is built for support. *Clinical Obstetrics and Gynecology*, 48(3):611–626, September 2005.

[31] Supreeth N. Gowda and Bruno Bordoni. *Anatomy, Abdomen and Pelvis, Levator Ani Muscle*, chapter 3, pages 286–293. StatPearls Publishing, 2021.

[32] Sender Herschorn. Female pelvic floor anatomy: the pelvic floor, supporting structures, and pelvic organs. *Reviews in urology*, 6(5):2–10, 2004.

[33] Keith Moore. *Clinically oriented anatomy*. Wolters Kluwer, Philadelphia, 2018.

[34] Peter Petros. *The female pelvic floor : function, dysfunction, and management according to the integral theory*. Springer, Heidelberg, 2007.

[35] G Davila. *Pelvic floor dysfunction : a multidisciplinary approach*. Springer, New York London, 2008.

[36] Ligaments of pelvis, Oct 2020. URL: https://epomedicine.com/medical-students/ligaments-of-pelvis/.

[37] Pedro T. Ramirez, Michael Frumovitz, and Nadeem R. Abu-Rustum. Chapter 2 - abdominal and pelvic anatomy. In *Principles of Gynecologic Oncology Surgery*, pages 3–49. Elsevier, 2018.

[38] Tamara A. Stein and John O. L. DeLancey. Structure of the perineal membrane in females. *Obstetrics & Gynecology*, 111(3):686–693, March 2008.

[39] Martin Pernoll. *Benson Pernoll's handbook of obstetrics gynecology*. McGraw-Hill, New York, 2001.

[40] Nouf Y. Akeel, Brooke Gurland, and Tracy Hull. Pelvic floor disorders related to urology and gynecology. *Obstet Gynecol Clin North*, pages 571–582, December 2018.

[41] Soo-Ho Chung and Woong Bin Kim. Various approaches and treatments for pelvic organ prolapse in women. *Journal of Menopausal Medicine*, 24(3):155, 2018.

[42] J Eric Jelovsek, Christopher Maher, and Matthew D Barber. Pelvic organ prolapse. *The Lancet*, 369(9566):1027–1038, March 2007.

[43] Matthew D. Barber and Christopher Maher. Epidemiology and outcome assessment of pelvic organ prolapse. *International Urogynecology Journal*, 24(11):1783–1790, October 2013.

[44] Antonio Simone Laganà, Valentina Lucia La Rosa, Agnese Maria Chiara Rapisarda, and Salvatore Giovanni Vitale. Pelvic organ prolapse: the impact on quality of life and psychological well-being. *Journal of Psychosomatic Obstetrics & Gynecology*, 39(2):164–166, March 2017.

[45] Robert E. Gutman, Daniel E. Ford, Lieschen H. Quiroz, Stuart H. Shippey, and Victoria L. Handa. Is there a pelvic organ prolapse threshold that predicts pelvic floor symptoms? *American Journal of Obstetrics and Gynecology*, 199(6):683.e1–683.e7, December 2008.

[46] C. Persu, C. R. Chapple, V. Cauni, S. Gutue, and P. Geavlete. Pelvic organ prolapse quantification system (pop-q) - a new era in pelvic prolapse staging. *Journal of medicine and life*, 4(1), March 2011.

[47] Yoshitaka Aoki, Heidi W. Brown, Linda Brubaker, Jean Nicolas Cornu, J. Oliver Daly, and Rufus Cartwright. Urinary incontinence in women. *Nature Reviews Disease Primers*, 3(1), July 2017.

[48] Isuzu Meyer and Holly E Richter. Impact of fecal incontinence and its treatment on quality of life in women. *Women's Health*, 11(2):225–238, March 2015.

[49] Patrick Y. H Lee and Scott R Steele. Complete pelvic floor repair in treating fecal incontinence. *Clinics in Colon and Rectal Surgery*, 18(01):55–59, February 2005.

[50] Alex Arnouk, Elise De, Alexandra Rehfuss, Carin Cappadocia, Samantha Dickson, and Fei Lian. Physical, complementary, and alternative medicine in the treatment of pelvic floor disorders. *Current Urology Reports*, 18(6), June 2017.

[51] William E. Whitehead and Adil E. Bharucha. Diagnosis and treatment of pelvic floor disorders: What's new and what to do. *Gastroenterology*, 138(4):1231–1235.e4, April 2010.

[52] Aboseif C. and Liu P. Pelvic organ prolapse. *StatPearls [Internet]*, October 2021.

[53] Rachel Y. K. Cheung, Jacqueline H. S. Lee, L. L. Lee, Tony K. H. Chung, and Symphorosa S. C. Chan. Vaginal pessary in women with symptomatic pelvic organ prolapse. *Obstetrics & Gynecology*, 128(1):73–80, July 2016.

[54] Friyan Turel Fatakia, Sarah Pixton, Jessica Caudwell Hall, and Hans Peter Dietz. Predictors of successful ring pessary use in women with pelvic organ prolapse. *Australian and New Zealand Journal of Obstetrics and Gynaecology*, 60(4):579–584, April 2020.

[55] Theerarat Yimphong, Teerayut Temtanakitpaisan, Pranom Buppasiri, Chompilas Chongsomchai, and Supparaluck Kanchaiyaphum. Discontinuation rate and adverse events after 1 year of vaginal pessary use in women with pelvic organ prolapse. *International Urogynecology Journal*, 29(8):1123–1128, August 2017.

[56] Kwang Jin Ko and Kyu-Sung Lee. Current surgical management of pelvic organ prolapse: Strategies for the improvement of surgical outcomes. *Investigative and Clinical Urology*, 60(6):413, 2019.

[57] Sybil G. Dessie, Alex Shapiro, Miriam J. Haviland, Michele R. Hacker, and Eman A. Elkadry. Obliterative versus reconstructive prolapse repair for women older than 70: Is there an optimal approach? *Female Pelvic Medicine & Reconstructive Surgery*, 23(1):23–26, January 2017.

[58] Naşide Mangir, Sabiniano Roman, Christopher R. Chapple, and Sheila MacNeil. Complications related to use of mesh implants in surgical treatment of stress urinary incontinence and pelvic organ prolapse: infection or inflammation? *World Journal of Urology*, 38(1):73–80, February 2019.

[59] Office of the Commissioner. Fda takes action to protect women's health, orders manufacturers of surgical mesh intended for transvaginal repair of pelvic organ prolapse to stop selling all devices. *U.S. Food and Drug Administration*, Apr 2019.

[60] Gabriela Coelho de Pinho Queirós. Análise computacional de imagens de ressonância magnética funcional. Master's thesis, FEUP, jul 2011.

[61] Geoffrey M. Currie, Peter Kamvosoulis, and Stewart Bushong. Pet/mri, part 2: Technologic principles. *Journal of Nuclear Medicine Technology*, 49(3):217–225, 2021.

[62] Edson Amaro Júnior and Helio Yamashita. Aspectos básicos de tomografia computadorizada e ressonância magnética. *Rev. Bras. Psiquiatr.*, 23(suppl 1):2–3, May 2001.

[63] Brian M Dale, Mark A Brown, and Richard C Semelka. *MRI basic principles and applications*. John Wiley & Sons, Ltd, Chichester, UK, October 2015.

[64] Camila Silva Boaventura, Daniel Padilha Rodrigues, Olimpio Antonio Cornehl Silva, Fabrício Henrique Beltrani, Rayssa Araruna Bezerra de Melo, Almir Galvão Vieira Bitencourt, Gustavo Gomes Mendes, and Rubens Chojniak. Evaluation of the indications for performing magnetic resonance imaging of the female pelvis at a referral center for cancer, according to the american college of radiology criteria. *Radiol. Bras.*, 50(1):1–6, January 2017.

[65] Courtney A Woodfield, Saravanan Krishnamoorthy, Brittany S Hampton, and Jeffrey M Brody. Imaging pelvic floor disorders: trend toward comprehensive MRI. *AJR Am. J. Roentgenol.*, 194(6):1640–1649, June 2010.

[66] Torsten ller. *Pocket atlas of sectional anatomy : computed tomography and magnetic resonance imaging. Volume II, Thorax, heart, abdomen, and pelvis*. Thieme, New York, 2014.

[67] Amar Khennane. *Introduction to finite element analysis using MATLAB and Abaqus*. CRC Press, Boca Raton, FL, 2013.

[68] Y. Bazilevs, V.M. Calo, J.A. Cottrell, J.A. Evans, T.J.R. Hughes, S. Lipton, M.A. Scott, and T.W. Sederberg. Isogeometric analysis using t-splines. *Computer Methods in Applied Mechanics and Engineering*, 199(5-8):229–263, January 2010.

[69] Ian A. Sigal, Hongli Yang, Michael D. Roberts, and J. Crawford Downs. Morphing methods to parameterize specimen-specific finite element model geometries. *Journal of Biomechanics*, 43(2):254–262, January 2010.

[70] Nathan Lauzeral, Domenico Borzacchiello, Michael Kugler, Daniel George, Yves Rémond, Alexandre Hostettler, and Francisco Chinesta. Shape parametrization of bio-mechanical finite element models based on medical images. *Computer Methods in Biomechanics and Biomedical Engineering: Imaging & Visualization*, 7(5-6):480–489, March 2018.

[71] Marco Evangelos Biancolini, Andrea Chiappa, Ubaldo Cella, Emiliano Costa, Corrado Groth, and Stefano Porziani. Radial basis functions mesh morphing. In Valeria V. Krzhizhanovskaya, Gábor Závodszky, Michael H. Lees, Jack J. Dongarra, Peter M. A. Sloot, Sérgio Brissos, and João Teixeira, editors, *Computational Science – ICCS 2020*, pages 294–308, Cham, 2020. Springer International Publishing.

[72] J. N. Reddy. *Introduction to the finite element method*. McGraw Hill Education, New York, NY, 2019.

[73] Singiresu Rao. *The finite element method in engineering*. Butterworth-Heinemann, an imprint of Elsevier, Kidlington, Oxford, United Kingdom, 2018.

[74] Maria Elisabete Teixeira da Silva. Estudo biomecânico de um feto durante um parto vaginal. Master's thesis, FEUP, jul 2012.

[75] R.A. Fontes Valente J. Pinho-da-Cruz F. Teixeira-Dias, R. J. de Alves de Sousa. *Método dos Elementos Finitos*. ETEP - Edições Técnicas e Profissionais, 2010.

[76] Matthew L Staten, Steven J Owen, Suzanne M Shontz, Andrew G Salinger, and Todd S Coffey. A comparison of mesh morphing methods for 3D shape optimization. In *Proceedings of the 20th International Meshing Roundtable*, pages 293–311. Springer Berlin Heidelberg, Berlin, Heidelberg, 2011.

[77] Rolland L Hardy. Multiquadric equations of topography and other irregular surfaces. *J. Geophys. Res.*, 76(8):1905–1915, March 1971.

[78] Ubaldo Cella, Corrado Groth, and Marco Biancolini. *Geometric Parameterization Strategies for shape Optimization Using RBF Mesh Morphing*, pages 537–545. Springer Science and Business Media LLC, 01 2017.

[79] Marco Evangelos Biancolini, Andrea Chiappa, Ubaldo Cella, Emiliano Costa, Corrado Groth, and Stefano Porziani. Radial basis functions mesh morphing. In Valeria V. Krzhizhanovskaya, Gábor Závodszky, Michael H. Lees, Jack J. Dongarra, Peter M. A. Sloot, Sérgio Brissos, and João Teixeira, editors, *Computational Science – ICCS 2020*, pages 294–308, Cham, 2020. Springer International Publishing.

[80] Corrado Groth, Stefano Porziani, Marco Biancolini, Emiliano Costa, Simona Celi, Katia Capellini, Michel Rochette, and Valery Morgenthaler. The medical digital twin assisted by reduced order models and mesh morphing. In *International CAE Conference*, 10 2018.

[81] Franck Mastrippolito, Stephane Aubert, Frédéric Ducros, and Martin Buisson. RBF-based mesh morphing improvement using schur complement applied to rib shape optimization. *International Journal of Numerical Methods for Heat & Fluid Flow*, 30(9):4241–4257, August 2019.

[82] Katia Capellini, Emiliano Costa, Marco Biancolini, Emanuele Vignali, Vincenzo Positano, Luigi Landini, and Simona Celi. An image-based and rbf mesh morphing cfd simulation for ataa hemodynamic. In *International CAE Conference*, 09 2017.

[83] Xiang Liu, Chao Han, Yingpu Cui, Tingting Xie, Xiaodong Zhang, and Xiaoying Wang. Detection and segmentation of pelvic bones metastases in mri images for patients with prostate cancer based on deep learning. *Frontiers in Oncology*, 11, 2021. URL: https://www.frontiersin.org/articles/10.3389/fonc.2021.773299, doi:10.3389/fonc.2021.773299.

[84] Seiichi Koshizuka, Kazuya Shibata, Masahiro Kondo, and Takuya Matsunaga. Chapter 4 - boundary conditions. In Seiichi Koshizuka, Kazuya Shibata, Masahiro Kondo, and Takuya Matsunaga, editors, *Moving Particle Semi-implicit Method*, pages 155–215. Academic Press, 2018. URL: https://www.sciencedirect.com/science/article/pii/B9780128127797000047, doi:https://doi.org/10.1016/B978-0-12-812779-7.00004-7.

[85] Robert C Pattinson, Anna Cuthbert, and Valerie Vannevel. Pelvimetry for fetal cephalic presentations at or near term for deciding on mode of delivery. *Cochrane Database Syst. Rev.*, 3(12):CD000161, March 2017.

[86] Jianping Niu, Juanmian Lei, and Jiandong He. Radial basis function mesh deformation based on dynamic control points. *Aerospace Science and Technology*, 64, 01 2017. doi: 10.1016/j.ast.2017.01.022.